Supporting Information

Fluorescence Turn-On Sensing of DNA Duplex Formation by a Tricyclic Cytidine Analogue

Dillon D. Burns, Kristine L. Teppang, Raymond W. Lee, Melissa E. Lokensgard, and Byron W. Purse*

Department of Chemistry and Biochemistry, San Diego State University, San Diego, California 92182, United States

e-mail: bpurse@mail.sdsu.edu

Contents

1. Materials and general methods

All reagents and chemicals used were purchased from Acros Organics and Fisher Chemical at ACS grade or higher quality and used as received without further purification, except as noted. 5-Amino-2-methylbenzothiazole was obtained from Alfa Aesar, 2-Cyanoethyl-N,N,N',N'-tetraisopropylphosphorodiamidite was obtained from Sigma-Aldrich. Solvents used for UV/vis and fluorescence measurements were spectrophotometric grade or were aqueous buffers prepared using Milli-Q water.

NMR (^{1}H and ^{13}C) spectra were acquired on Varian 400 MHz and a Varian 500 MHz NMR spectrometers and recorded at 298 K. Chemical shifts are referenced to the residual protio solvent peaks and given in parts per million (ppm). Splitting patterns are denoted as s (singlet), d (doublet), dd (doublet of doublet), t (triplet), q (quartet), and m (multiplet). Fluorescence measurements were recorded on a PTI Quantamaster QM-400 fluorescence spectrophotometer and corrected using the manufacturer's calibration files. Absorbance measurements were taken on a Shimadzu Pharma Spec 1700 UV-Vis spectrophotometer. CD spectroscopy was performed on an Aviv Model 420 and recorded at 298 K. High-resolution electrospray ionization (ESI) mass spectrometry was performed at the University of California, Riverside High Resolution Mass Spectrometry Facility using an Agilent LC-TOF in ESI mode.

Synthetic steps that required an inert atmosphere were carried out under dried nitrogen gas using standard Schleck techniques.

2. Synthesis and characterization of novel compounds

Synthetic scheme of (**1**) (8-DEA)tC

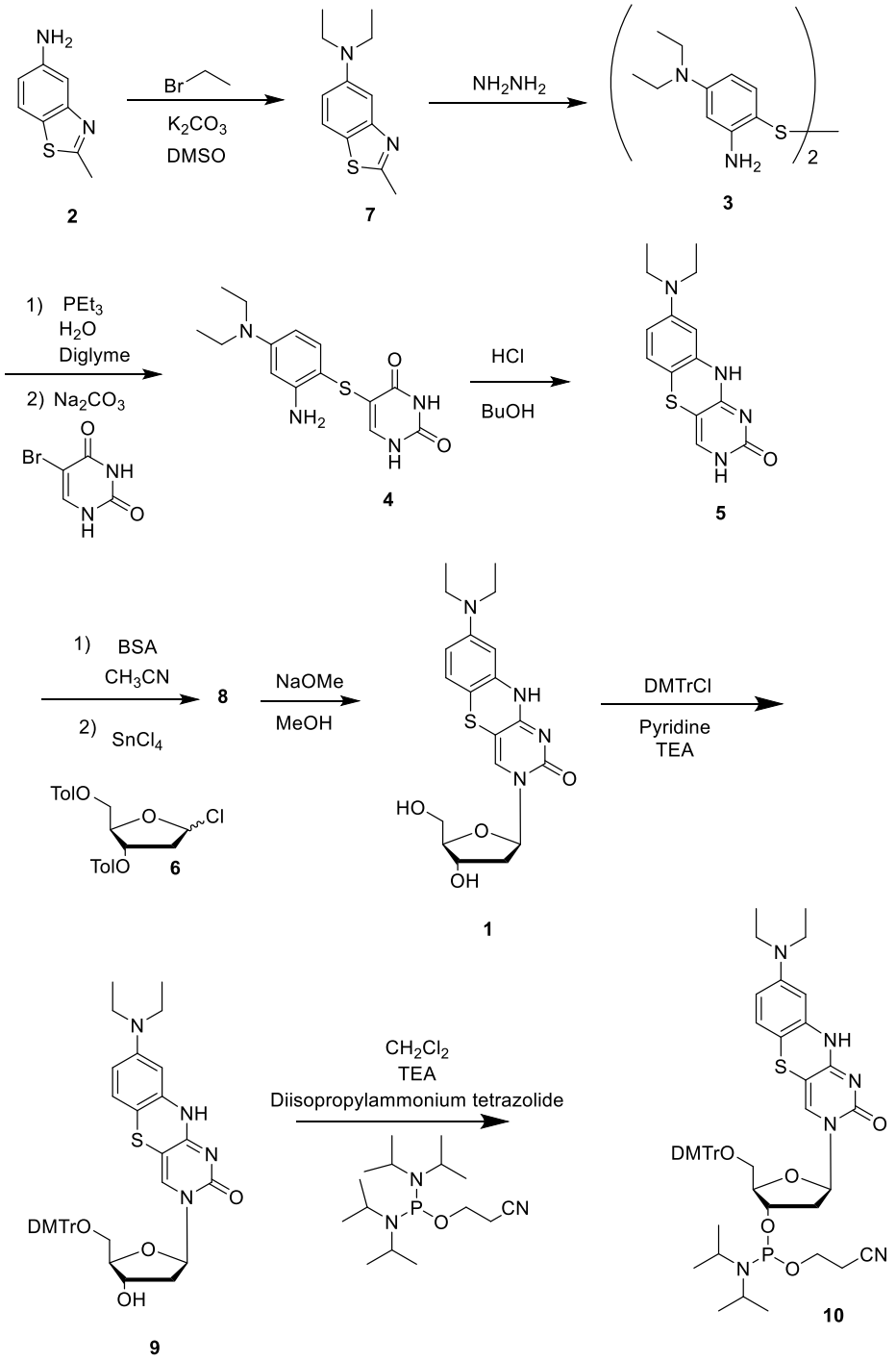

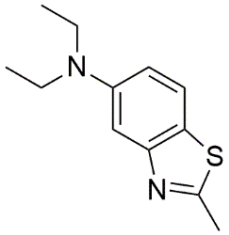

5-Diethylamino-2-methylbenzothiazole 7. 5-Amino-2-methylbenzothiazole **2** (5.58 g; 29.0 mmol) was placed in a dry 3 necked 100mL round bottomed flask under nitrogen. To this was added a minimal amount of DMSO to achieve dissolution and the resulting mixture was stirred for 5 minutes. Anhydrous potassium carbonate was added to the reaction (3.26; 58 mmol) and bromoethane (4.33 mL, 58 mmol) and the reaction was heated to 80°C and monitored by TLC (10% MeOH in dichloromethane). The reaction was found to be complete at 3 days. The reaction mixture was then diluted with and water extracted with ethyl acetate. The organics were combined and dried over sodium sulfate before solvent removal. Flash chromatography was performed using a gradient from hexane to ethyl acetate (0-100%) to yield the pure product as a yellow oil (5.1g, 80%). ^{1}H NMR (400 MHz,$CDCl_3$): δ 7.44 (d, J=8.9 Hz, 1H), 7.16 (d, J=2.5 Hz, 1H), 6.66 (d, J=8.9 Hz, 1H), 3.25 (m, J=7.1 Hz, 4H), 1.50 (t, J=7.0 Hz, 6H) ^{13}C NMR (100 MHz, $CDCl_3$): δ 173.2, 148.7, 148.4, 121.8, 115.2, 113.8, 101.2, 44.9, 19.0, 12.2. (ESI) cald. for $C_{12}H_{17}N_2S$ [M+H]+ 221.1112, found 221.1106

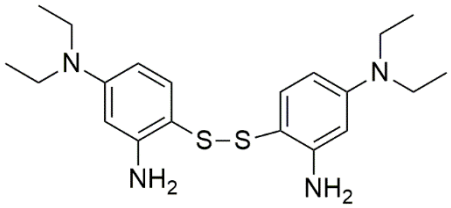

2-[(2-Amino-4-diethylaminophenyl)disulfanyl]-5-diethylaminoaniline 3. 5-Diethylamino-2-methylbenzothiazole **7** (4.1 g, 18.6mmol) was placed in a dry 100 mL round-bottomed flask under nitrogen. To this was added 25 mL of hydrazine hydrate and the reaction mixture was stirred at room temperature for ten minutes. The reaction mixture was then heated at 100 °C for 18hrs. The reaction was monitored by TLC (10% MeOH in DCM) and found to be complete at 18 hours. The reaction was cooled to room temperature and rotovapped to dryness, then the product was extracted with EtOAC (3X). The organics were combined and dried over anhydrous sodium sulfate before evaporating to dryness. The product was purified by flash chromatography (1% MeOH in DCM). The pure product was found to be a yellow solid. (2.89g, 79.5%) ^{1}H NMR (500 MHz,$CDCl_3$): δ 7.08 (d, J=8.4 Hz, 2H), 6.00 (m, 4H), 4.25 (s, 4H), 3.32 (q, J=7.1 Hz, 8H), 1.15 (t, J=7.1 Hz, 12H) ^{13}C NMR (100 MHz, $CDCl_3$): δ 150.7, 149.9, 138.6, 106.0, 103.1, 96.9, 44.3, 12.7. Due to this compound's propensity for oxidative degradation, no mass spectrum was obtained for this intermediate.

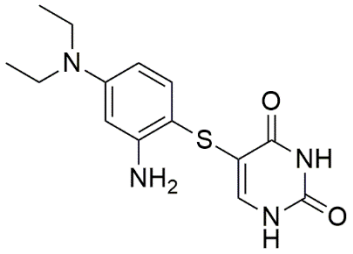

5-[(2-Amino-4-diethylaminophenyl)sulfanyl]pyrimidine-2,4(1*H*,3*H*)-dione 4. 2-[(2-Amino-5-diethylaminol)disulfanyl]-5-diethylaminoaniline **3** (1.4g, 3.6mmol) was placed in a dry 3 neck 100mL round-bottomed flask under nitrogen, to this was added triethylphosphine (1.79mL of a 1M solution in THF) and water (32.0 uL). The reaction was stirred for 5 minutes at room temperature (25°C). 5-Bromouracil (1.37g, 7.2mmol) and sodium carbonate (0.603g, 7.2mmol) were added to the reaction mixture and stirred at 120 °C. The reaction was monitored by TLC (10% MeOH in DCM) and found to be complete at 18 hours. Upon completion the reaction mixture was cooled to room temperature and the resulting precipitate was filtered and rinsed with several portions of water and a few portions of ether. The material was purified by flash chromatography (0-10% MeOH in DCM). The solvent was removed by rotary evaporation. The product was found to be an off-white solid (800mg, 36%) ^{1}H NMR (400 MHz, $(CD_3)_2SO$): δ 11.27 (s, 1H), 10.91 (s, 1H), 7.14 (s, 1H), 7.11 (d, J= 8.6Hz, 1H), 6.02 (d, J=2.7Hz, 1H), 5.93 (dd, J=8.7, 2.7Hz, 1H), 5.25 (d, J=8.4 Hz, 1H), 3.31 (m, 1H), 3.24 (m, 4H), 1.06 (t, J=6.9Hz, 6H). (ESI) cald. for $C_{14}H_{18}N_4O_2S$ [M+H]+ 307.1150, found 307.1237

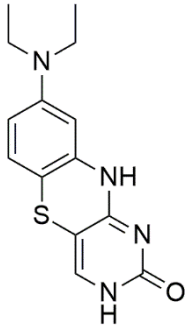

8-Diethylamino-3*H*-pyrimido[5,4-*b*][1,4]benzothiazin-2(10*H*)-one 5. 5-[(2-Amino-4-diethylaminophenyl)sulfanyl]pyrimidine-2,4(1*H*,3*H*)-dione **4** (800mg, 2.61mmol) was placed in a clean dry 50 mL round-bottomed flask under N_2. To this was added 15mL of 1-butanol and the reaction was heated to 120 °C for 10 minutes and then cooled to room temperature. Once cooled, concentrated HCl (1.5mL) was added to the reaction and the reaction mixture was heated to 120 °C. The reaction was monitored by TLC (10%MeOH in DCM) and found to be complete at 24 hrs. Upon completion the reaction was cooled to room temp and quenched with 5% ammonium hydroxide. The reaction mixture was evaporated to dryness and the crude product was purified by flash chromatography to yield a yellow solid (0.733g, 97%) ^{1}HNMR (400MHz, $(CD_3)_2SO$): δ 10.87 (s, 1H), 9.87 (s, 1H), 7.32 (s, 1H), 6.77 (d, J=8.6 Hz, 1H), 6.41 (d, J=2.4 Hz, 1H), 6.27 (dd, J=8.7, 2.4 Hz, 1H), 3.23 (m, 4H), 1.51 (t, J=6.9 Hz, 6H) ^{13}C

NMR (100 MHz, $(CD_3)_2SO$): δ 161.5, 155.9, 147.3, 137.8, 137.1, 126.9, 107.8, 100.7, 99.7, 94.8, 44.1, 12.6. (ESI) cald. for $C_{14}H_{16}N_4OS$ [M+H]+ 289.1045, found 289.1162.

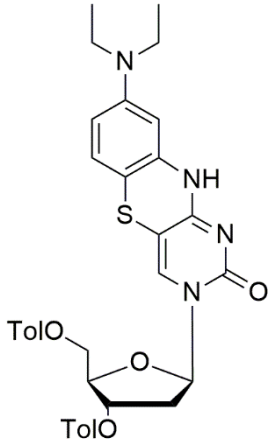

8-Diethylamino-tC 3',5'-di-*O*-(*p*-toluoyl)-2'-deoxy-*β*-D-ribonucleoside 8. 8-Diethylamino-3*H*-pyrimido[5,4-*b*][1,4]benzothiazin-2(10*H*)-one **5** (346.1 mg, 1.2 mmol) was suspended in dry acetonitrile in a Schlenk tube under nitrogen. Bis(trimethylsilyl)acetamide (1.38 mmol) was added and the reaction mixture allowed to stir at 50 °C for 1 h until the starting material had completely dissolved and reacted to form the TMS ether, as indicated by a color change to orange. The reaction mixture was allowed to cool to room temperature and 3',5'-di-*O*-(*p*-toluoyl)-2'-deoxy-*α*-D-ribofuranosyl chloride (1.32 mmol) was added with stirring. The reaction mixture was cooled to 0 °C and tin(IV) chloride (0.24mmol) was added dropwise. The reaction mixture was stirred at 0 °C, then allowed to warm to room temperature, and the progress was tracked by TLC (10% CH_3OH in CH_2Cl_2). The reaction was complete in 45 min. At this time, the mixture was diluted with ethyl acetate (40 mL), washed with a saturated, aqueous solution of $NaHCO_3$ (40 mL), and dried over Na_2SO_4. Rotary evaporation followed by purification of the semi-crude material containing both the α and β anomers. The product was isolated as a yellow powder (0.76g, 86%). This semi-crude product was carried over into the subsequent deprotection reaction.

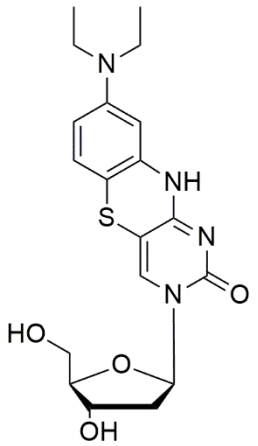

8-Diethylamino-tricyclic-2'-deoxy-*β*-D-ribonucleoside 1. 8-Diethylamino-tC 3',5'-di-*O*-(*p*-toluoyl)-2'-deoxy-*β*-D-ribonucleoside **8** (662 mg, 1.03 mmol) was placed in a dry 25mL round-bottomed flask and suspended in 5 mL of methyl alcohol. To this was added (0.769 mL, 4.13 mmol) of 25% NaOMe in methanol and the reaction was tracked by TLC (10%MeOH in CH_2Cl_2) and found to be complete in 18 hrs. The reaction was quenched by the addition of acetic acid (.236mL, 4.13mmol) and the solvent was removed by rotary evaporation. Purification and separation of the α and β anomers was done using flash chromatography and 10% EtOH in $CHCl_3$. The products were isolated as separate anomers in the form of yellow films (168.3mg total, 39% yield of each of the α and β anomers) ^{1}H NMR (400 MHz, MeOD): δ 7.88 (s, 1H), 6.77 (d, J=8.7Hz, 1H), 6.35 (dd, J=8.5, 2.6Hz, 1H), 6.32 (d, J=2.5Hz, 1H), 6.19 (t, J=6.4Hz, 1H), 4.36 (m, 1H), 3.92 (q, J=3.5Hz, 1H), 3.82 (dd, J=12.1, 3.1Hz, 1H), 3.72 (dd, J=12.0, 3.6Hz, 1H), 3.34 (m, 4H), 2.35 (m, 1H), 2.14 (m, 1H), 1.14 (t, J=6.9Hz, 6H) ^{13}C NMR (100 MHz, MeOD): δ 160.6, 156.1, 147.6, 136.7, 134.1, 126.3, 108.3, 100.6, 100.1, 98.7, 87.6, 86.4, 70.3, 61.1, 48.4, 44.0, 11.4. (ESI) cald. for $C_{19}H_{24}N_4O_4S$ [M+H]+ 405.1518, found 405.1623.

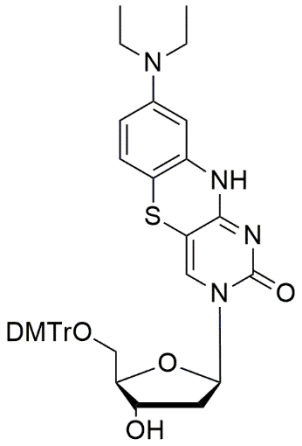

8-Diethylamino-tC 2'-deoxy-5'-dimethoxytrityl-*β*-D-ribonucleoside 9. 8-Diethylamino-tricyclic-2'-deoxy-*β*-D-ribonucleoside **1** (129 mg, 3.18 mmol) was placed in a clean dry 25mL side-armed, round-bottomed flask. To this was added a minimal amount of dry pyridine (about 3mL) under N_2 and dry triethylamine (48.7 µL, 3.50 mmol) was then added, and the reaction mixture stirred for 5 minutes. To this was added dimethoxytritylchloride (118 mg, 3.50 mmol) and the reaction was monitored by TLC (10% MeOH in CH_2Cl_2) and found to be complete in 3 hours. The reaction was quenched with MeOH and the solvent was evaporated by rotary evaporation. The crude product was purified by flash chromatography (10% MeOH in CH_2Cl_2 with 1% triethylamine). The semi-crude product retained a small amount of dimethoxytrityl impurity but was carried directly into the next reaction. ^{1}H NMR (400 MHz, $CDCl_3$): δ 7.64 (s, 1H), 7.43 (m, 2H), 7.31 (m, 6H), 7.21 (t, J=7.3, 1H), 6.84 (m, 4H), 6.68 (d, J=8.7 Hz, 1H), 6.28 (t, J=6.3 Hz, 1H), 6.26 (m, 1H), 6.12 (d, J=2.6 Hz, 1H), 4.48 (m, 1H), 4.09 (m, 1H), 3.77 (s, 3H), 3.76 (s, 3H), 3.77 (m, 2H), 3.29 (q, J=7.1 Hz, 4H), 2.64 (m, 1H), 2.23 (m, 1H), 1.13 (t, J=7.0 Hz, 6H).

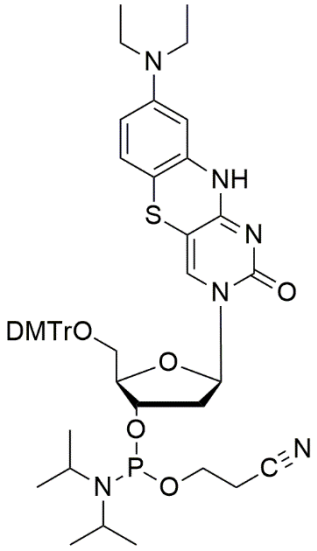

8-Diethylamino-tC 2'-deoxy-5'-dimethoxytrityl-3'-cyanoethyldiisopropylphosphoramidite-*β*-D-ribonucleoside 10. 8-Diethylamino-tC 2'-deoxy-5'-dimethoxytrityl-*β*-D-ribonucleoside **9** (all crude material from the previous step) was placed in a dry 25mL side-armed, round-bottomed flask under N_2. To this was added diisopropylammonium tetrazolide (0.152 mg, 4 eq.) and anhydrous CH_2Cl_2 (2 mL). The reaction mixture was stirred for five minutes, and then 2-cyanoethyl-*N*,*N*,*N*',*N*'-tetraisopropylphosphorodiamidite was added (77.5 µL, 0.244 µmol). The reaction was monitored by TLC (10% MeOH in CH_2Cl_2) and found to be complete in 2.5 hours. The solvent was evaporated by rotary evaporation and the crude product was purified by flash chromatography (0 to 100% EtOAc in hexanes with 1% trimethylamine to protect the compound from the acidic nature of the silca). The product was isolated as a yellow film in a mixture of two diastereomers (120mg, 45% over two steps). ^{1}H NMR (400 MHz, $CDCl_3$): δ 7.71 and 7.65 (s, 1H), 7.42 (m, 2H), 7.30 (m, 6H), 7.21 (m, 1H), 6.83 (m, 4H), 6.66 (m, 1H), 6.27 (m, 2H), 6.01 (m, 1H), 4.55 (m, 1H), 4.10 (m, 1H), 3.77 and 3.76 (m, 6H), 3.58 (m, 4H), 3.42 and 3.34 (m, 2H), 3.28 (q, J=7.1 Hz, 4H), 2.75 and 2.64 (m, 1H), 2.61 and 2.42 (t, J=6.5 Hz, 2H), 2.24 (m, 1H), 1.22-1.04 (m, 12H), 1.06 (t, J=7.0 Hz, 6H). ^{31}P NMR (162 MHz, $CDCl_3$): 150.0 149.8: (ESI) cald. for $C_{49}H_{59}N_6O_7PS$ [M+H]+ 907.3904, found 907.3951.

3. Oligonucleotide synthesis and characterization

Solid phase DNA synthesis to prepare oligonucleotides containing 8-DEA-tC was performed by TriLink BioTechnologies, San Diego, CA using standard phosphoramidite conditions and compound 8-DEA-tC amidite **10**. The HPLC-purified oligonucleotides were characterized by MALDI-TOF mass spectrometry and found to match the expected molecular weights as shown below. Natural DNA oligonucleotides for the complementary sequences and the AA mismatch and AA complement with the dSpacer abasic site surrogate were obtained from Integrated DNA Technologies, Coralville, IA.

Sequence Name	Sequence	Expected Molecular Weight (g/mol)	Mass Spec Analysis (amu)
GA	5'-CGC-A**G**X-**A**TC-G-3'	3190.7	3190.1
CT	5'-CGC-A**C**X-**T**TC-G-3'	3141.8	3140.9
GC	5'-CGC-A**G**X-**C**TC-G-3'	3166.7	3166.5
CA	5'-CGC-A**C**X-**A**TC-G-3'	3150.8	3150.0
GG	5'-CGC-A**G**X-**G**TC-G-3'	3206.7	3206.2
CC	5'-CGC-A**C**X-**C**TC-G-3'	3126.8	3126.0
TA	5'-CGC-A**T**X-**A**TC-G-3'	3165.8	3165.2
TT	5'-CGC-A**T**X-**T**TC-G-3'	3156.8	3156.1
AA	5'-CGC-A**A**X-**A**TC-G-3'	3174.8	3174.2

Complementary Sequences

Sequence Name	Sequence
GA complement	5'-CGA-TGC-TGC-G-3'
CT complement	5'-CGA-AGG-TGC-G-3'
GC complement	5'-CGA-GGC-TGC-G-3'
CA complement	5'-CGA-TGG-TGC-G-3'
GG complement	5'-CGA-CGC-TGC-G-3'
CC complement	5'-CGA-GGG-TGC-G-3'
TA complement	5'-CGA-TGA-TGC-G-3'
TT complement	5'-CGA-AGA-TGC-G-3'
AA complement	5'-CGA-TGT-TGC-G-3'
AA mismatch complement	5'-CGA-TAT-TGC-G-3'
AA abasic site complement	5'-CGA-T(dSpacer)T-TGC-G-3'

4. Computational details and molecular modeling of (8-DEA)tC in a DNA duplex

Calculations were carried out under Gaussian 09[1] using the B3LYP density functional method[2,3] and the cc-pVDZ basis set.[4] Geometries were optimized to default convergence criteria, and a natural bond order (NBO) analysis[5] carried out on the molecular orbitals at the optimized geometry. The HOMO and LUMO were rendered using GaussView 5.0.[6]

tC energy and optimized geometry.

Energy = -1444.05026047 hartree

Atomic Number	Coordinates (Angstroms) X	Y	Z
6	2.568452	0.641700	-0.490761
6	3.517709	0.821847	0.696449
6	4.226099	-0.989618	-0.721768
6	4.783728	0.143063	0.166525
1	3.130176	0.268019	1.565560
1	3.655504	1.876678	0.964726
1	4.768668	-0.974689	-1.682397
8	2.832185	-0.669164	-0.966426
6	4.292709	-2.382293	-0.110458
1	5.349024	-2.668315	0.016865
1	3.832733	-3.105585	-0.811455
8	3.698309	-2.448115	1.177191
1	2.754005	-2.269075	1.056554
8	5.535344	0.995233	-0.695666
1	5.823322	1.761315	-0.177220
1	5.410445	-0.259188	0.981751
7	1.136144	0.747608	-0.171967
6	0.315514	-0.337786	-0.135880
6	0.651214	2.068162	0.091469
6	-1.010488	-0.198472	0.165432
1	0.779830	-1.297617	-0.354356
8	1.450526	2.993807	0.092291
7	-0.698986	2.206846	0.304322
6	-1.477494	1.147084	0.340928
16	-2.069802	-1.601326	0.470652
7	-2.820697	1.377408	0.533882
6	-3.644872	-0.878070	0.027454
6	-3.858632	0.508688	0.159056
1	-3.043172	2.367765	0.581549
6	-4.697770	-1.711682	-0.362220
6	-5.136445	1.027545	-0.095573
6	-5.972281	-1.187777	-0.594436
1	-4.513475	-2.782262	-0.473442
6	-6.188929	0.185266	-0.457259
1	-5.299567	2.104721	-0.004076
1	-6.787779	-1.851991	-0.885855

1	2.777571	1.398616	-1.264010
1	-7.177678	0.609765	-0.641147

8-DEA-tC energy and optimized geometry.

Energy = -1656.64869984 hartree

Atomic Number	Coordinates (Angstroms) X	Y	Z
6	-4.095977	0.766006	0.461013
6	-5.062165	0.931451	-0.714855
6	-5.865898	-0.708574	0.854128
6	-6.360619	0.390628	-0.110359
1	-4.738644	0.291011	-1.550027
1	-5.128197	1.971927	-1.056432
1	-6.378955	-0.575057	1.822042
8	-4.445879	-0.481397	1.040974
6	-6.056924	-2.135734	0.360054
1	-7.135369	-2.346871	0.280622
1	-5.633556	-2.834796	1.107236
8	-5.506978	-2.350365	-0.930875
1	-4.548379	-2.238809	-0.846473
8	-7.028761	1.360408	0.695081
1	-7.264069	2.106609	0.123799
1	-7.034392	-0.025393	-0.879934
7	-2.670123	0.736044	0.102282
6	-1.931189	-0.407931	0.142151
6	-2.098340	1.988750	-0.284485
6	-0.608393	-0.395749	-0.201212
1	-2.457140	-1.308123	0.454141
8	-2.828158	2.969702	-0.343270
7	-0.750042	2.007162	-0.543050
6	-0.050613	0.892166	-0.506175
16	0.339190	-1.890873	-0.419445
7	1.297743	1.007196	-0.753928
6	1.968675	-1.241436	-0.063470
6	2.283832	0.101795	-0.323053
1	1.584905	1.971826	-0.892203
6	2.990561	-2.087469	0.374295
6	3.593944	0.566269	-0.149781
6	4.297706	-1.636762	0.532887
1	2.760322	-3.133956	0.586144
6	4.637331	-0.282732	0.286559
1	3.782407	1.615367	-0.370958
1	5.047839	-2.349562	0.868056
7	5.931206	0.201007	0.500190
6	7.051870	-0.740688	0.481710
6	6.203796	1.604033	0.175226
1	7.913824	-0.248849	0.950615
1	6.815430	-1.586676	1.143137
6	7.438334	-1.250053	-0.912364
1	6.136118	1.786045	-0.918795
1	5.405944	2.206508	0.636606

6	7.536988	2.139974	0.693392
1	6.598169	-1.774367	-1.394118
1	7.741869	-0.420517	-1.572205
1	8.285541	-1.952633	-0.844155
1	7.648285	1.964242	1.775396
1	8.407237	1.706280	0.177858
1	7.568725	3.227613	0.523661
1	-4.225743	1.591865	1.179395

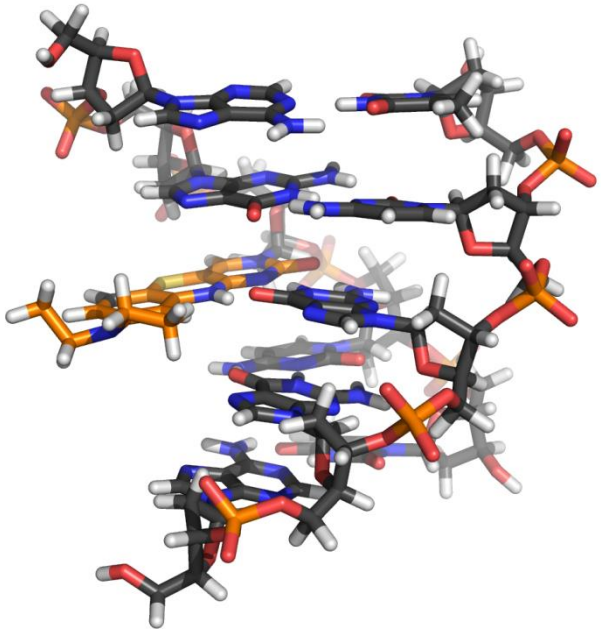

Figure S1. 8-DEA-tC in the sequence 5′-AG(8-DEA-tC)CT-3′ hybridized to its complement. The 8-DEA-tC molecule (orange C atoms) protrudes into the major groove where there is ample space for the diethylamino group to rotate freely. Molecular model prepared using Spartan ’08 with the default structural parameters for B form DNA. The native atoms of the natural DNA were held frozen and the geometry of the additional atoms of the 8-DEA-tC nucleobase was optimized using molecular mechanics and the MMFF force field.

5. UV/Vis, fluorescence spectra and quantum yield determinations

All photophysical experiments were measured in a quartz sub-micro cuvette (10 mm path length) purchased from Starnacell Inc. Solutions were prepared in 1X PBS buffer at pH 7.4. Steady state emission scans were recorded using a PTI QuantaMaster QM-400 and absorbances were measured on a Shimadzu UV-1700 Pharmaspec spectrometer. Quantum yield measurements were performed the comparative method of Williams *et. al.* and measured in duplicate, at minimum.[7] Quinine sulfate in 0.1M H_2SO_4 was used as a reference standard for all photophysical measurements. We validated the measurements by using a commercial sample of pyrrolo-dC and obtaining a fluorescence quantum yield of 0.046, matching the value of 0.05 as reported by the Tor group.[8] All measurements were taken with an absorbance range of 0.01-0.1. Subsequent dilutions were performed stepwise in order to obtain a minimum of five absorbance and emission spectra for quantum yield determinations. *Representative data from these quantum yield measurements is plotted below.* Quantum yield determinations were obtained using the following equation:

$$\Phi_{\mathrm{X}} = \Phi_{\mathrm{Std}} \left(\frac{\mathrm{Slope_X}}{\mathrm{Slope_{Std}}}\right)\left(\frac{{\eta_{\mathrm{X}}}^2}{{\eta_{\mathrm{Std}}}^2}\right)$$

The determination of quantum yields for single-stranded oligonucleotides containing 8-DEA tC were calculated using the integrated emission intensity measurements of the single strand prior to the addition of the complementary strand, with the following equation. This method was validated by comparison with and confirmed with a SS quantum yield experiment.

$$SS\,\Phi = DS\,\Phi \times \frac{SS\,EMInitial}{DS\,EMInitial} \times \frac{DS\,ABS}{SS\,ABS} \times \frac{DS\,Total\,Vol}{SS\,Total\,Vol}$$

Samples of double-stranded oligonucleotides were prepared using a known concentration of single-stranded oligonucleotide and adding a total of 2.4 equivalents of complementary strand at room temperature. A single-strand absorbance and emission were taken prior to the addition of the first 1.2 equivalents of complementary strand for purposes of single-strand calculation and verification of hybridization. An additional 1.2 equivalent is added after the first double-strand to ensure that complete hybridization was achieved. Thermal annealing procedures had no effect on the measurements as expected, given that these sequences were chosen to have no competing, stable secondary structures.

Normalized absorption and emission plots of single-stranded oligonucleotides and double-stranded oligonucleotides in 1X PBS buffer at pH 7.4 are shown below. Note: ***Not all normalized quantum yields are drawn to the same scale.***

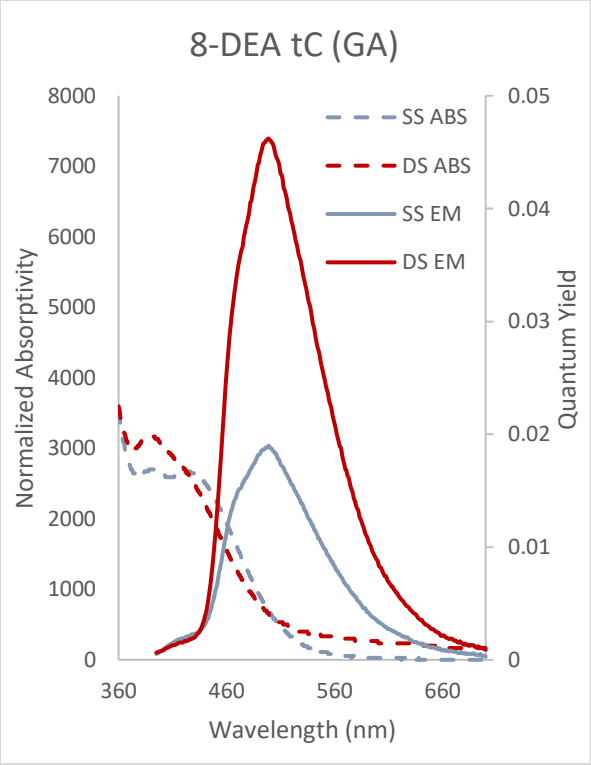

Figure S2. Absorption and emission plots of 8-DEA tC (GA) in 1X PBS at 23°C.

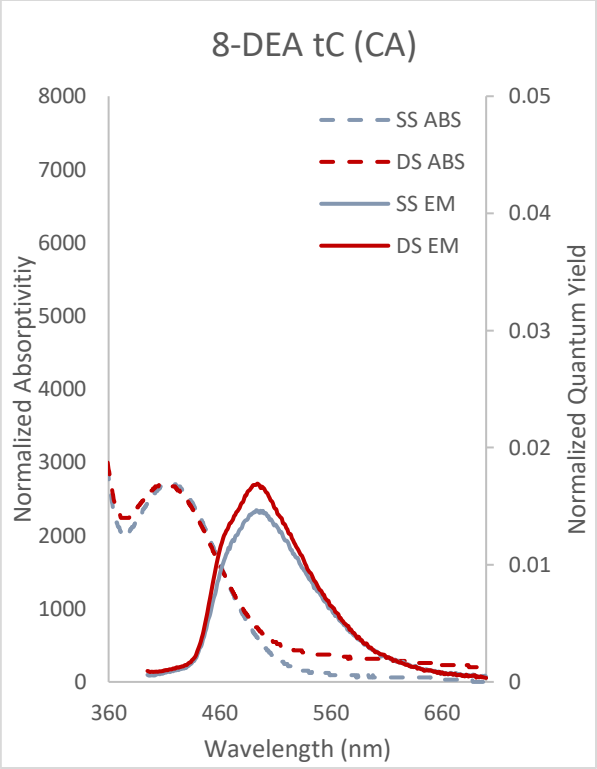

Figure S3. Absorption and emission plots of 8-DEA tC (CA) in 1X PBS at 23°C.

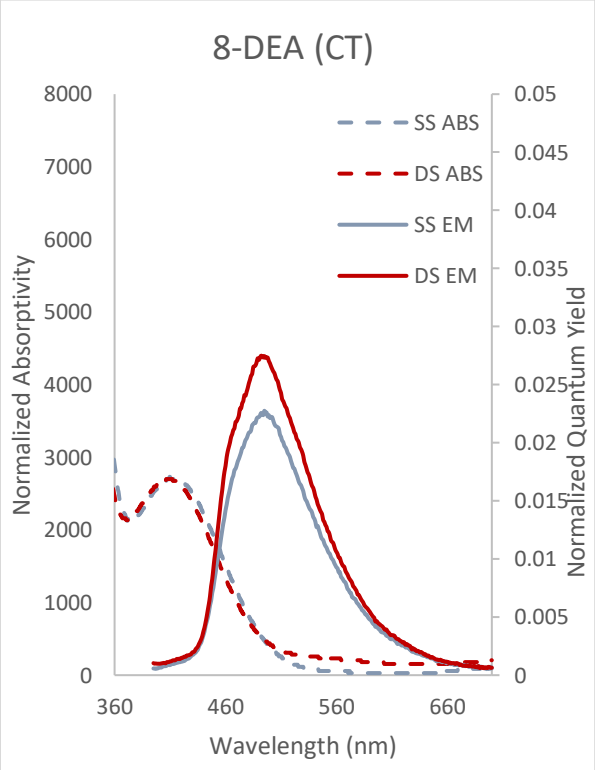

Figure S4. Absorption and emission plots of 8-DEA tC (CT) in 1X PBS at 23°C.

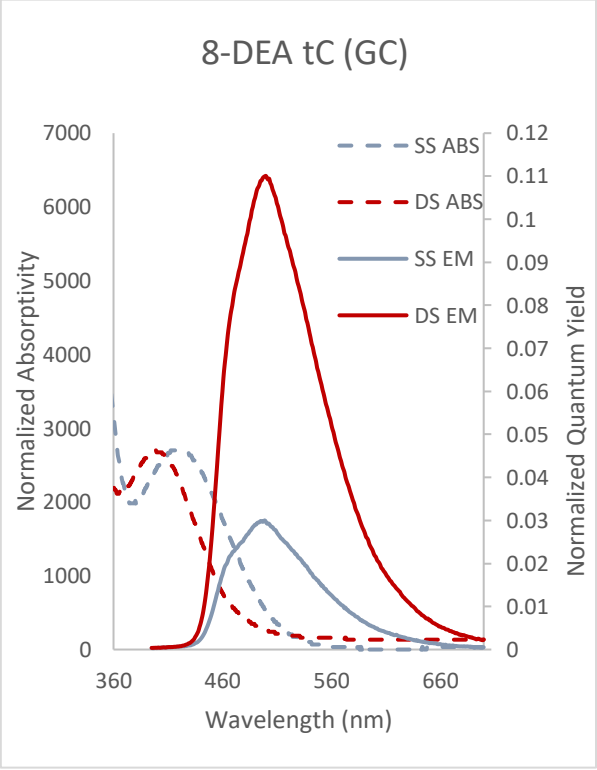

Figure S5. Absorption and emission plots of 8-DEA tC (GC) in 1X PBS at 23°C.

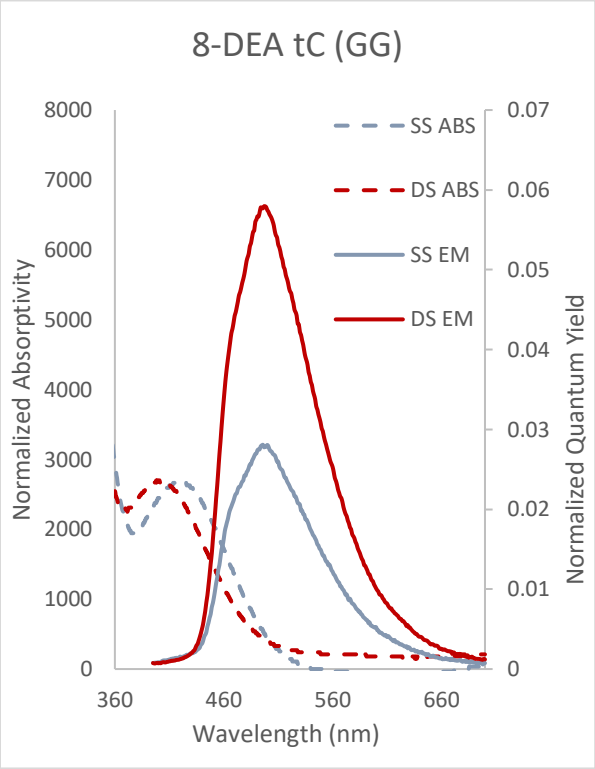

Figure S6. Absorption and emission plots of 8-DEA tC (GG) in 1X PBS at 23°C.

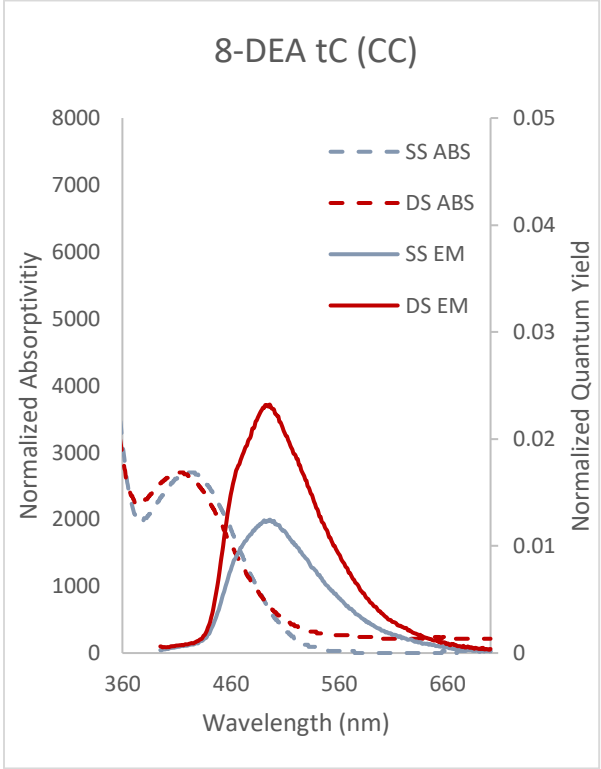

Figure S7. Absorption and emission plots of 8-DEA tC (CC) in 1X PBS at 23°C.

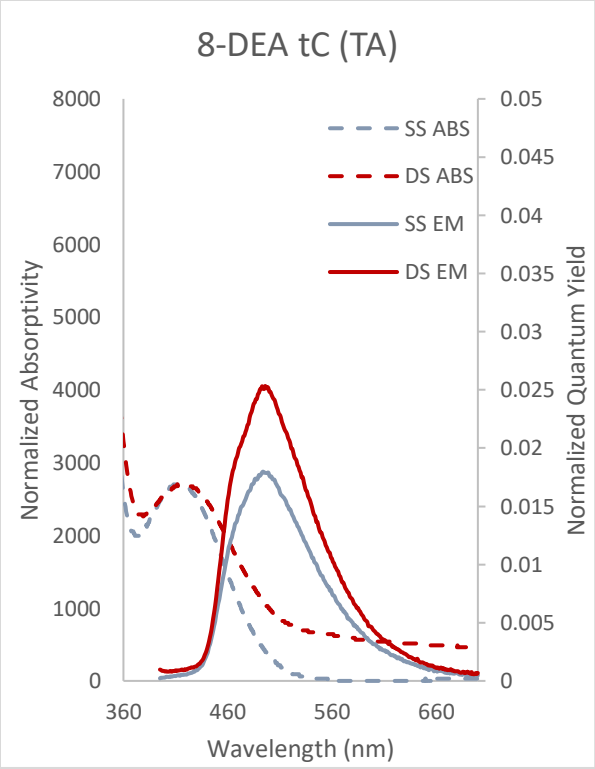

Figure S8. Absorption and emission plots of 8-DEA tC (TA) in 1X PBS at 23°C.

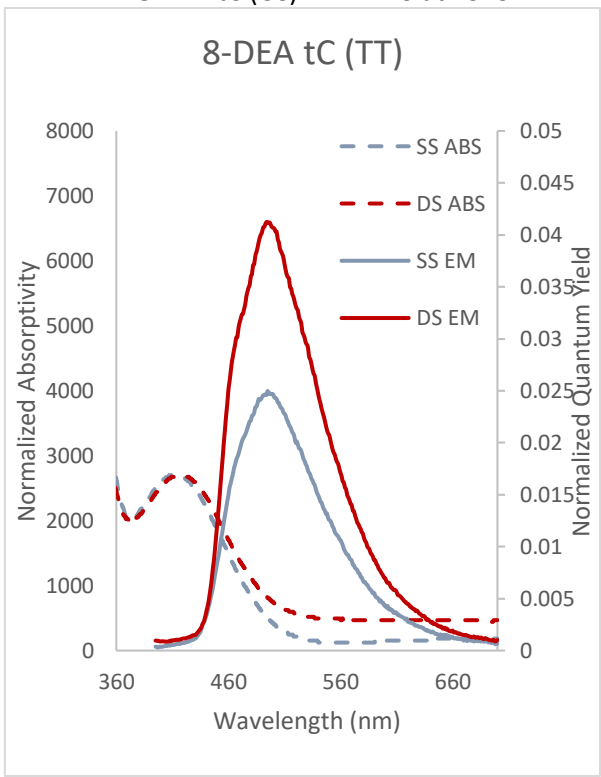

Figure S9. Absorption and emission plots of 8-DEA tC (TT) in 1X PBS at 23°C.

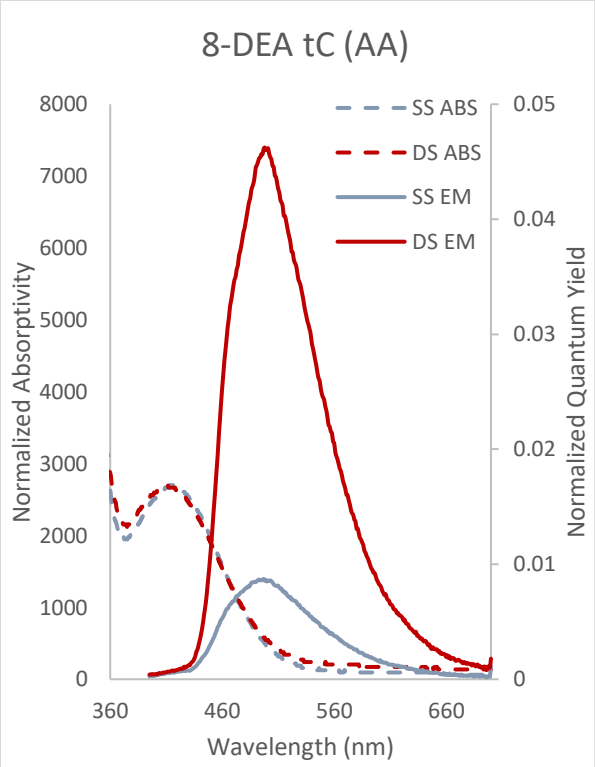

Figure S10. Absorption and emission plots of 8-DEA tC (AA) in 1X PBS at 23°C.

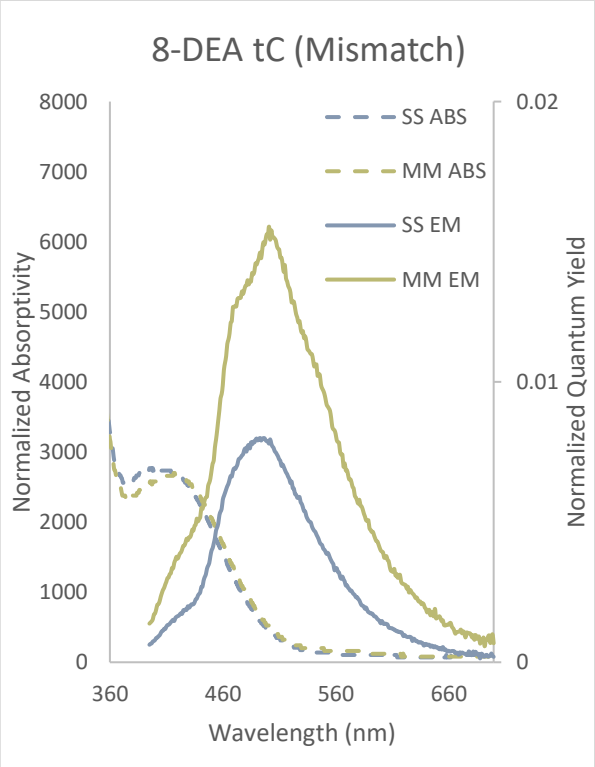

Figure S11. Absorption and emission plots of 8-DEA tC (MM) in 1X PBS at 23°C.

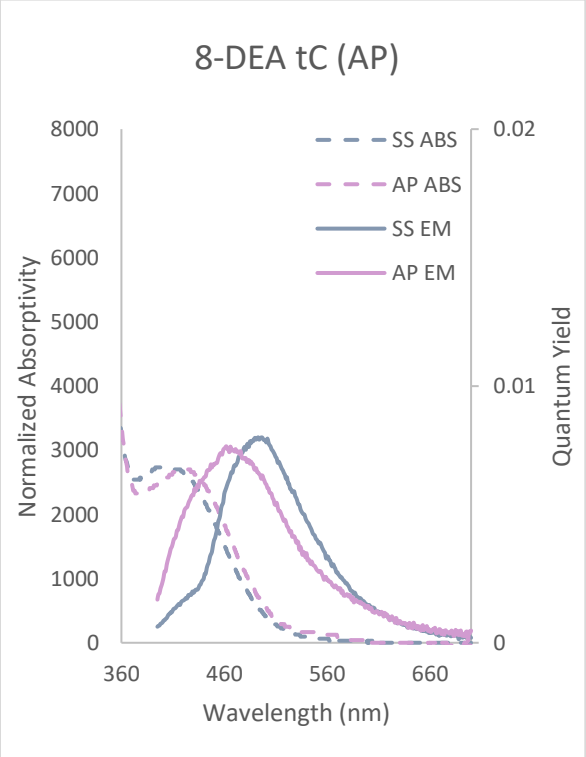

Figure S12. Absorption and emission plots of 8-DEA tC (AP) in 1X PBS at 23°C.

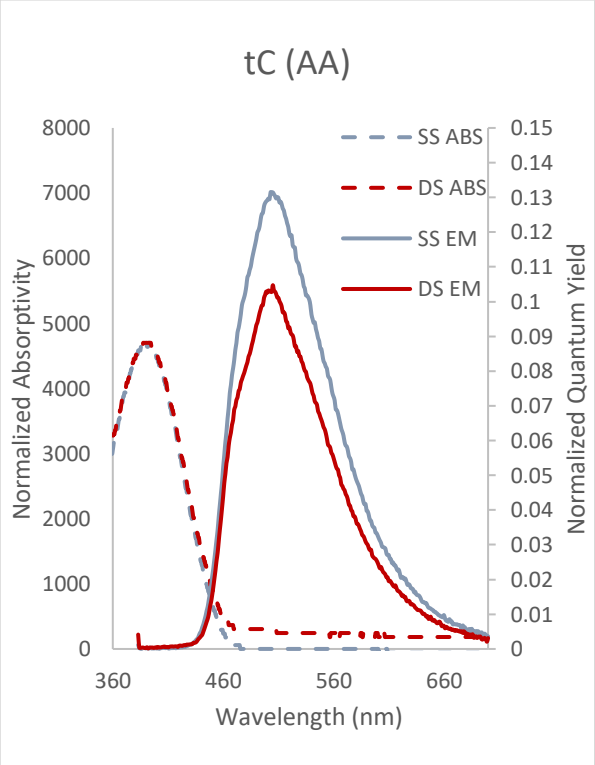

Figure S13. Absorption and emission plots of tC (AA) in 1X PBS at 23°C.

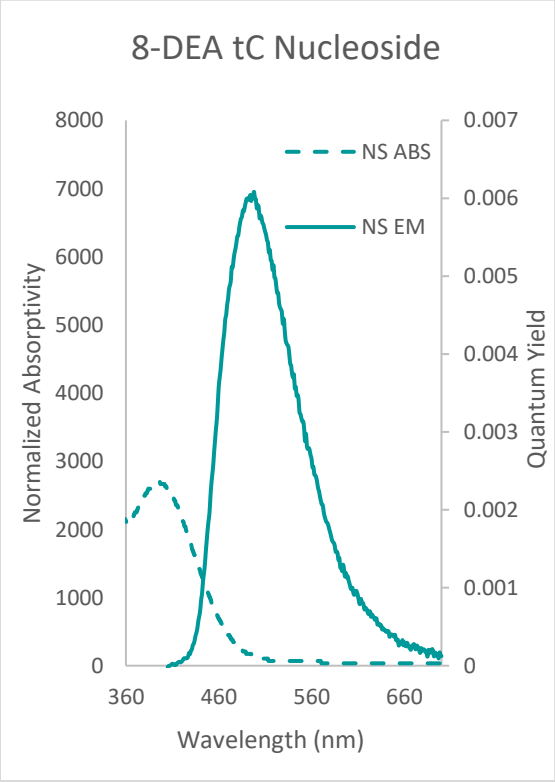

Figure S14. Absorption and emission plots of 8-DEA tC Nucleoside in 1X PBS at 23°C.

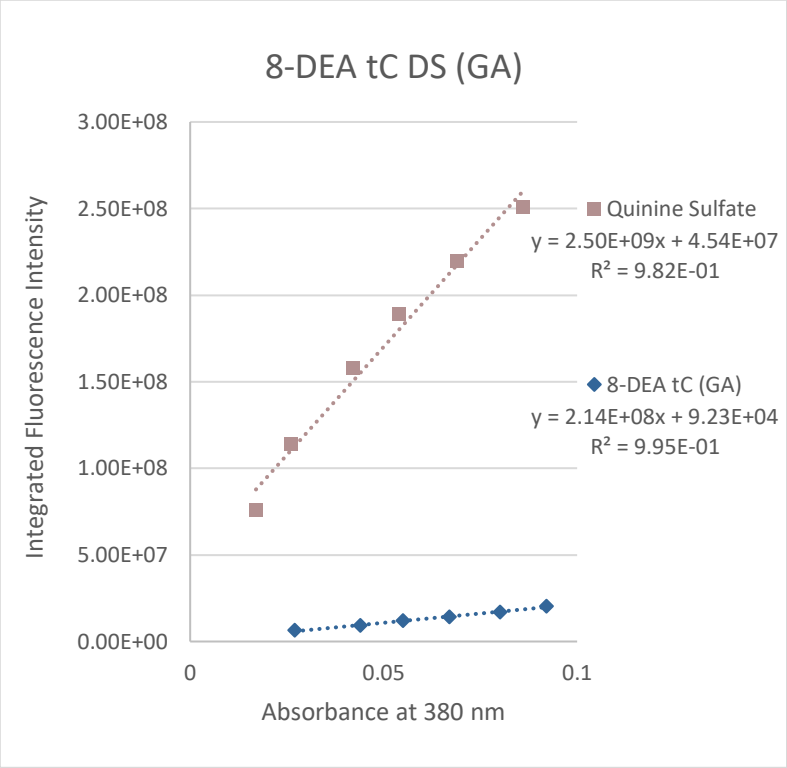

Quinine Sulfate		8-DEA tC (GA)	
Absorbance (380 nm)	Integrated Emission	Absorbance (380 nm)	Integrated Emission
0.086	2.51E+08	0.092	2.03E+07
0.069	2.19E+08	0.08	1.70E+07
0.054	1.89E+08	0.067	1.42E+07
0.042	1.58E+08	0.055	1.19E+07
0.026	1.14E+08	0.044	9.19E+07
0.017	7.54E+07	0.027	7.54E+07

Figure S15. Quantum Yield determination plot and data table of 8-DEA tC DS (GA) in 1X PBS Buffer at 23°C.

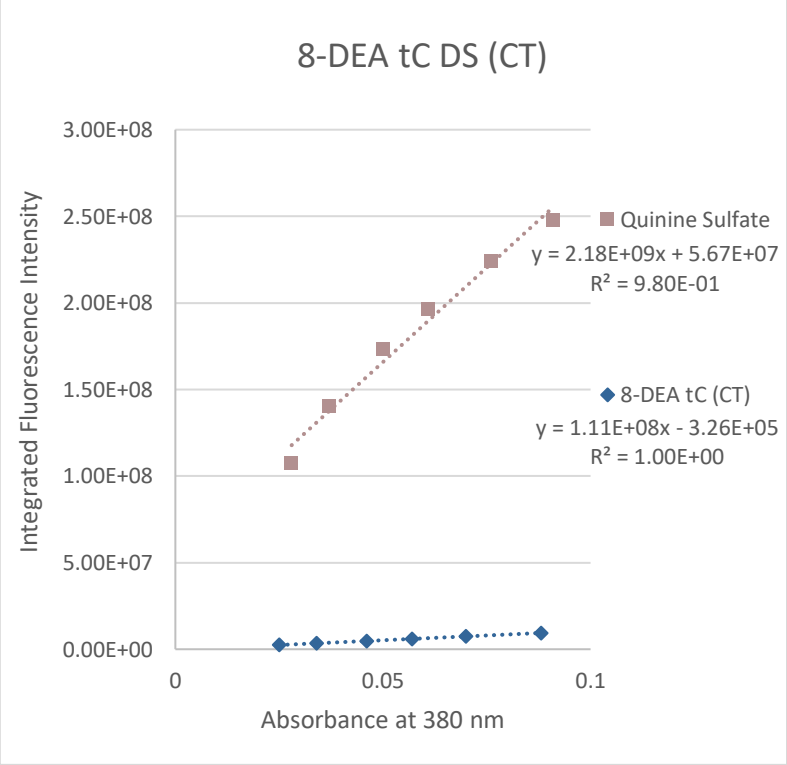

Quinine Sulfate		8-DEA tC (CT)	
Absorbance (380 nm)	Integrated Emission	Absorbance (380 nm)	Integrated Emission
0.091	2.48E+08	0.088	9.37E+06
0.076	2.24E+08	0.070	7.50E+06
0.061	1.96E+08	0.057	5.97E+06
0.050	1.73E+08	0.046	4.69E+06
0.037	1.40E+08	0.034	3.42E+06
0.028	1.07E+08	0.025	2.48E+06

Figure S16. Quantum Yield determination plot and data table of 8-DEA tC DS (CT) in 1X PBS Buffer at 23°C.

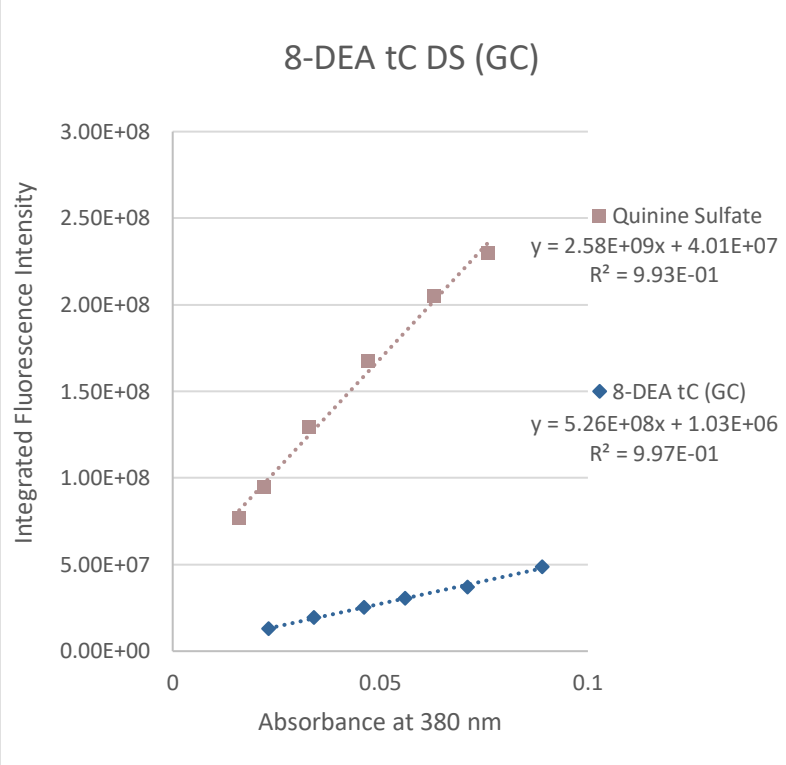

Quinine Sulfate		8-DEA tC (GC)	
Absorbance (380 nm)	Integrated Emission	Absorbance (380 nm)	Integrated Emission
0.076	2.30E+08	0.089	4.86E+07
0.063	2.05E+08	0.071	3.72E+07
0.047	1.68E+08	0.056	3.06E+07
0.033	1.29E+08	0.046	2.53E+07
0.022	9.47E+07	0.034	1.94E+07
0.028	7.67E+07	0.025	1.30E+07

Figure S17. Quantum Yield determination plot and data table of 8-DEA tC DS (GC) in 1X PBS Buffer at 23°C.

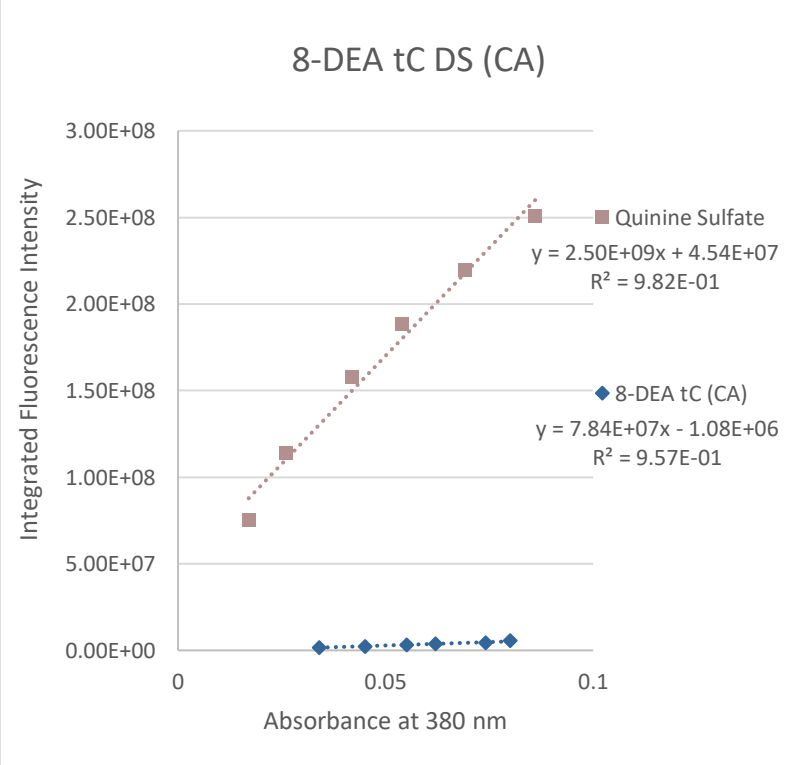

Quinine Sulfate		8-DEA tC (CA)	
Absorbance (380 nm)	Integrated Emission	Absorbance (380 nm)	Integrated Emission
0.086	2.51E+08	0.080	5.66E+06
0.069	2.19E+08	0.074	4.35E+06
0.054	1.89E+08	0.062	3.66E+06
0.042	1.58E+08	0.055	3.15E+06
0.026	1.14E+08	0.045	2.39E+06
0.017	7.54E+07	0.034	1.78E+06

Figure S18. Quantum Yield determination plot and data table of 8-DEA tC DS (CA) in 1X PBS Buffer at 23°C.

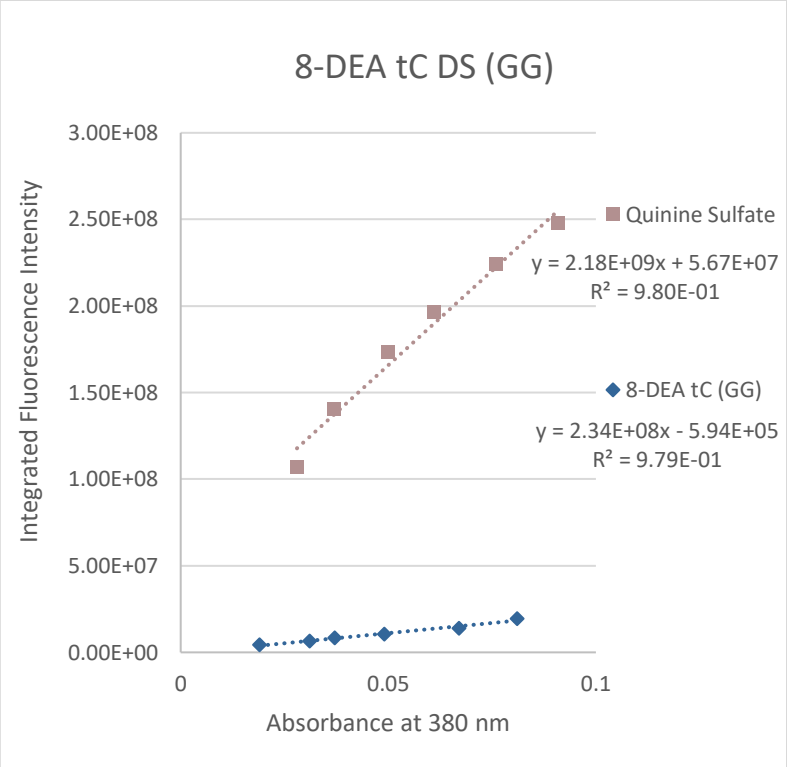

Quinine Sulfate		8-DEA tC (GG)	
Absorbance (380 nm)	Integrated Emission	Absorbance (380 nm)	Integrated Emission
0.091	2.48E+08	0.081	1.95E+07
0.076	2.24E+08	0.067	1.39E+07
0.061	1.96E+08	0.049	1.05E+07
0.050	1.73E+08	0.037	8.26E+06
0.037	1.40E+08	0.031	6.42E+06
0.028	1.07E+08	0.019	4.40E+06

Figure S19. Quantum Yield determination plot and data table of 8-DEA tC DS (GG) in 1X PBS Buffer at 23°C.

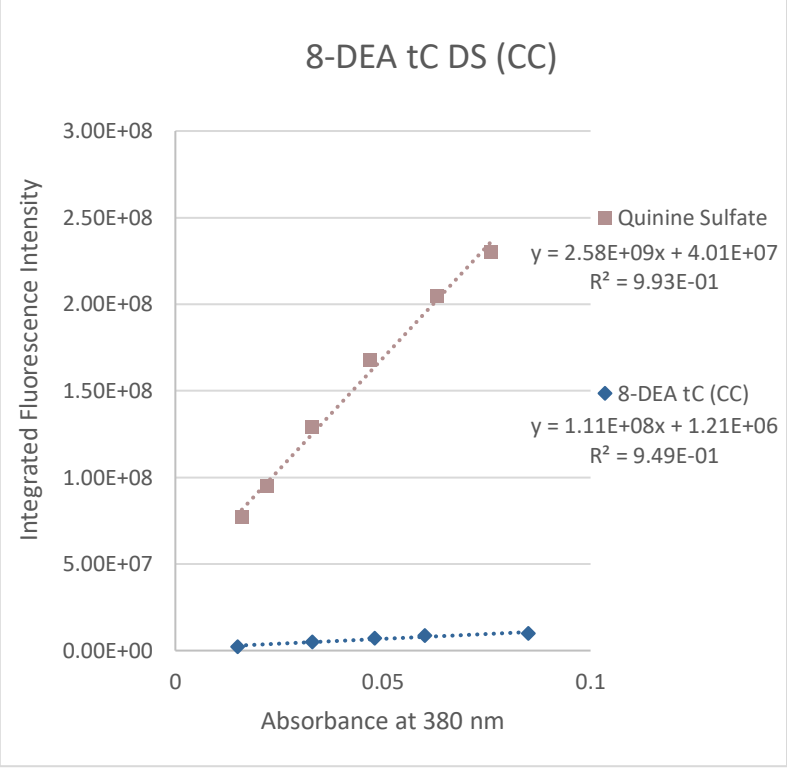

Quinine Sulfate		8-DEA tC (CC)	
Absorbance (380 nm)	Integrated Emission	Absorbance (380 nm)	Integrated Emission
0.091	2.48E+08	0.081	1.95E+07
0.076	2.24E+08	0.067	1.39E+07
0.061	1.96E+08	0.049	1.05E+07
0.050	1.73E+08	0.037	8.26E+06
0.037	1.40E+08	0.031	6.42E+06
0.028	1.07E+08	0.019	4.40E+06

Figure S20. Quantum Yield determination plot and data table of 8-DEA tC DS (CC) in 1X PBS Buffer at 23°C.

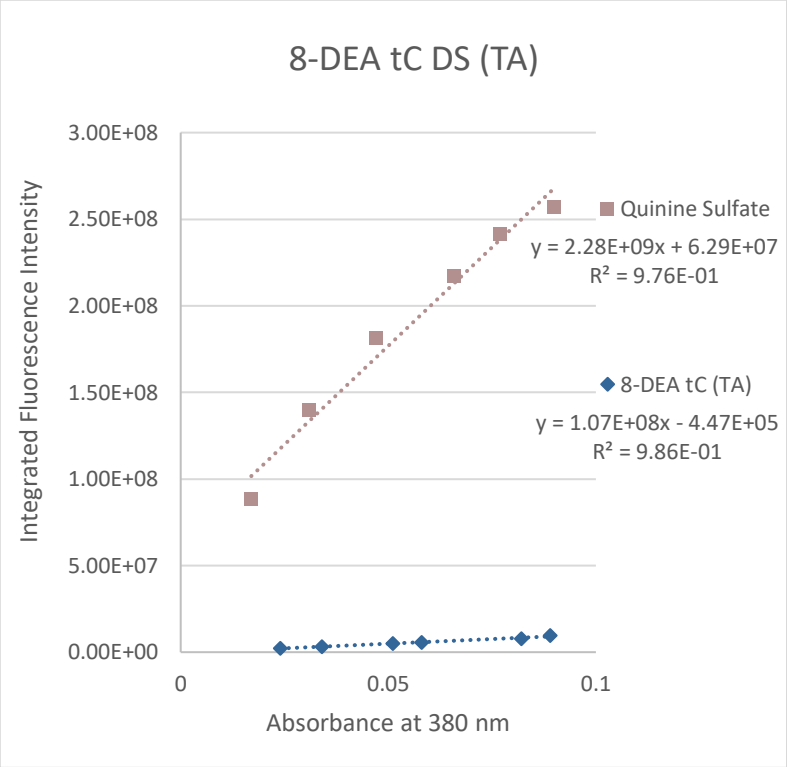

Quinine Sulfate		8-DEA tC (TA)	
Absorbance (380 nm)	Integrated Emission	Absorbance (380 nm)	Integrated Emission
0.090	2.57E+08	0.089	9.62E+06
0.077	2.41E+08	0.082	7.84E+06
0.066	2.17E+08	0.058	5.76E+06
0.047	1.82E+08	0.051	4.92E+06
0.031	1.40E+08	0.034	3.22E+06
0.017	8.81E+07	0.024	2.24E+06

Figure S21. Quantum Yield determination plot and data table of 8-DEA tC DS (TA) in 1X PBS Buffer at 23°C.

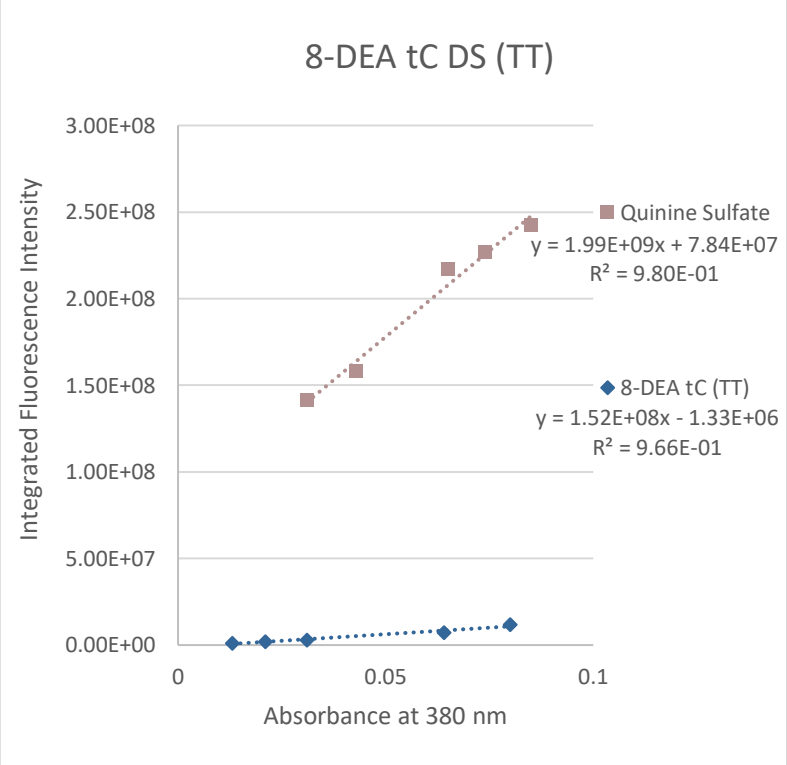

Quinine Sulfate		8-DEA tC (TT)	
Absorbance (380 nm)	Integrated Emission	Absorbance (380 nm)	Integrated Emission
0.085	2.42E+08	0.080	1.18E+07
0.074	2.27E+08	0.064	7.31E+06
0.065	2.17E+08	0.031	2.82E+06
0.043	1.58E+08	0.021	1.96E+06
0.031	1.41E+08	0.013	1.21E+06

Figure S22. Quantum Yield determination plot and data table of 8-DEA tC DS (TT) in 1X PBS Buffer at 23°C.

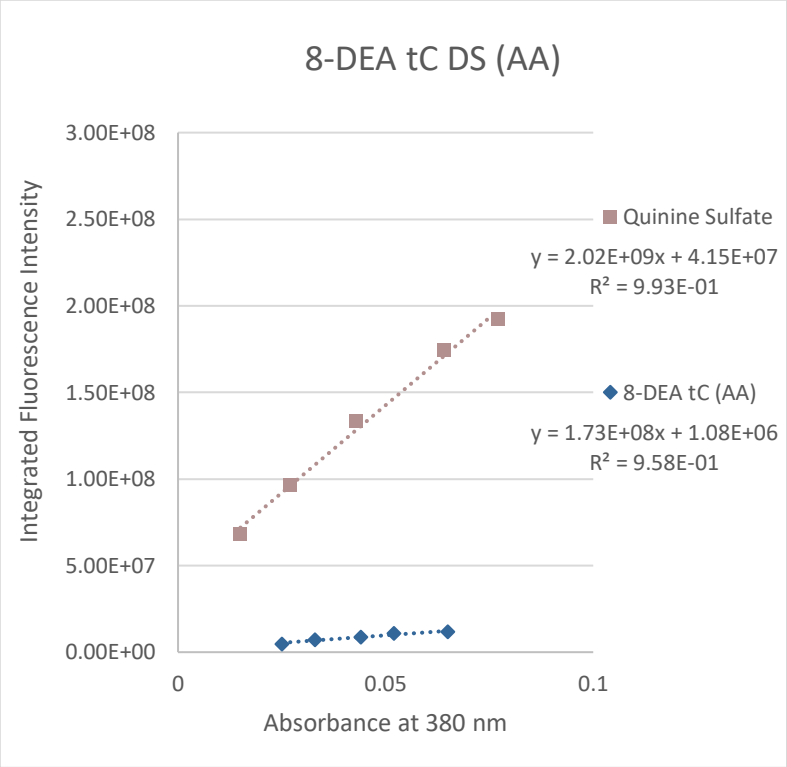

Quinine Sulfate		8-DEA tC (AA)	
Absorbance (380 nm)	Integrated Emission	Absorbance (380 nm)	Integrated Emission
0.077	1.92E+08	0.077	1.18E+08
0.064	1.74E+08	0.064	7.31E+08
0.043	1.33E+08	0.043	2.82E+08
0.027	9.63E+07	0.027	1.96E+07
0.015	6.83E+07	0.015	1.21E+07

Figure S23. Quantum Yield determination plot and data table of 8-DEA tC DS (AA) in 1X PBS Buffer at 23°C.

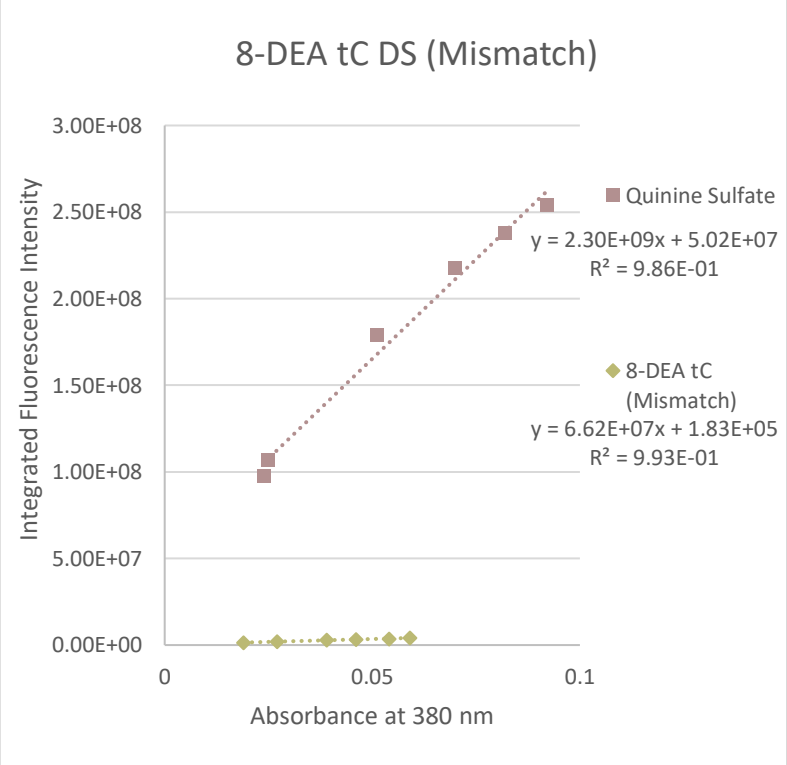

Quinine Sulfate		8-DEA tC (Mismatch)	
Absorbance (380 nm)	Integrated Emission	Absorbance (380 nm)	Integrated Emission
0.092	2.54E+08	0.059	4.11E+06
0.082	2.38E+08	0.054	3.62E+06
0.07	2.18E+08	0.046	3.33E+06
0.051	1.79E+08	0.039	2.85E+06
0.025	1.07E+08	0.027	1.96E+06
0.024	9.75E+07	0.029	1.39E+06

Figure S24. Quantum Yield determination plot and data table of 8-DEA tC (Mismatch) in 1X PBS Buffer at 23°C.

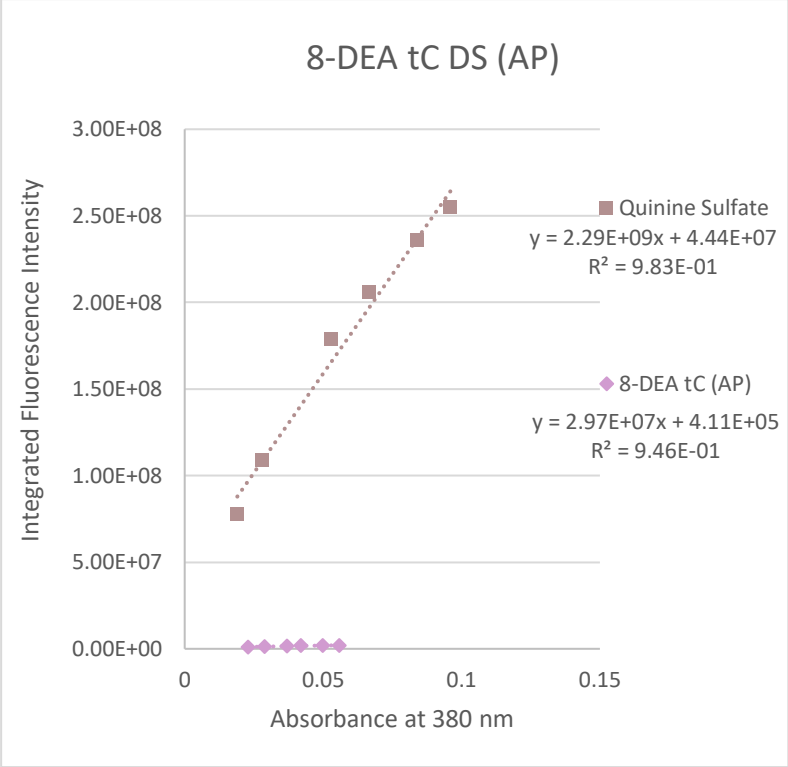

Quinine Sulfate		8-DEA tC (AP)	
Absorbance (380 nm)	Integrated Emission	Absorbance (380 nm)	Integrated Emission
0.096	2.55E+08	0.056	1.97E+06
0.084	2.36E+08	0.050	1.95E+06
0.067	2.06E+08	0.042	1.80E+06
0.053	1.78E+08	0.037	1.48E+06
0.028	1.09E+08	0.029	1.29E+06
0.019	7.78E+07	0.023	1.03E+06
		0.021	8.56E+05

Figure S25. Quantum Yield determination plot and data table of 8-DEA tC (AP) in 1X PBS Buffer at 23°C.

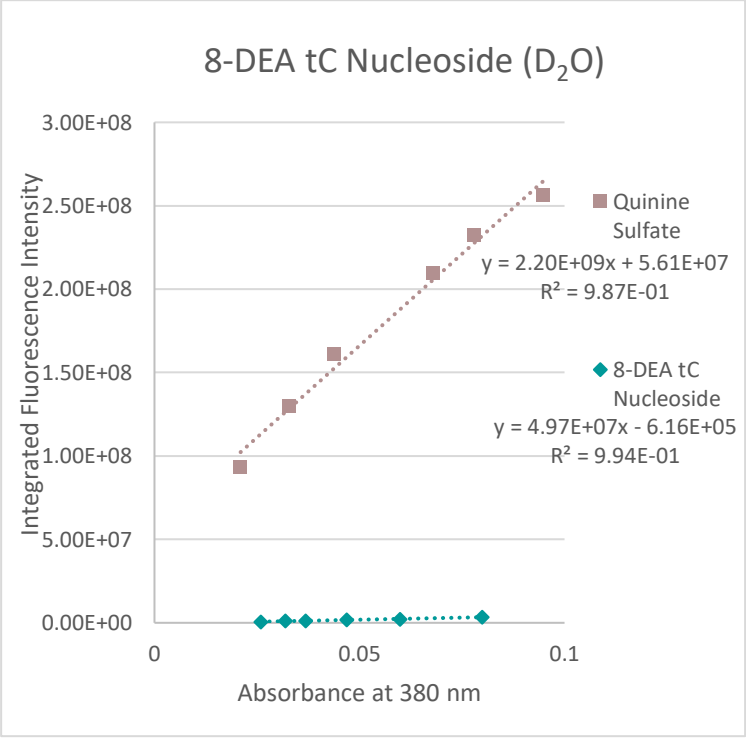

Quinine Sulfate		8-DEA tC Nucleoside (D_2O)	
Absorbance (380 nm)	Integrated Emission	Absorbance (380 nm)	Integrated Emission
0.095	2.56E+08	0.080	3.41E+06
0.078	2.32E+08	0.060	2.23E+06
0.068	2.10E+08	0.047	1.74E+06
0.044	1.61E+08	0.037	1.30E+06
0.033	1.30E+08	0.032	1.02E+06
0.021	9.33E+07	0.026	6.16E+06
		0.021	4.28E+05

Figure S26. Quantum Yield determination plot and data table of 8-DEA tC (Nucleoside) in D_2O at 23°C.

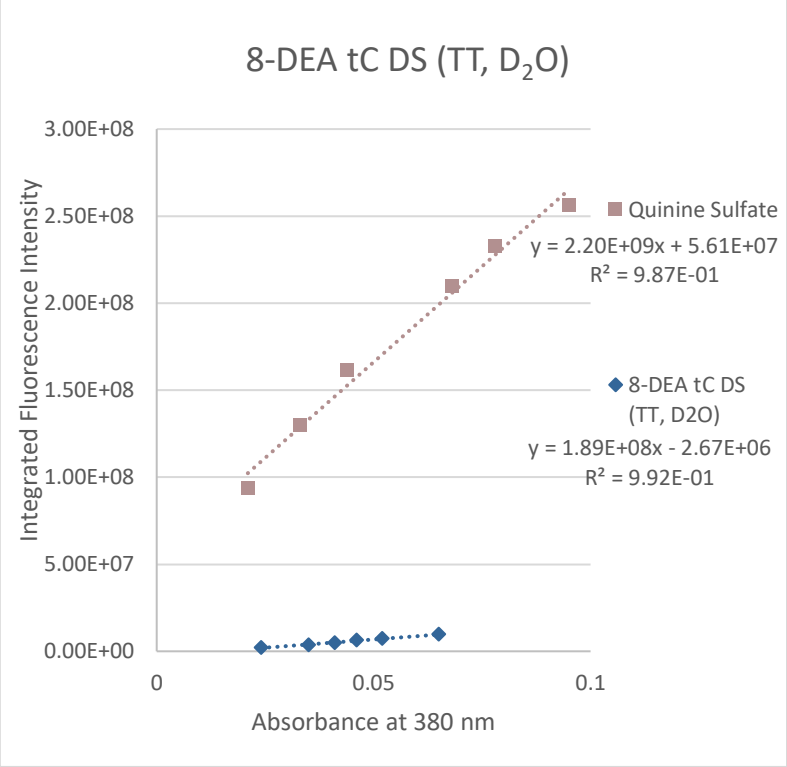

Quinine Sulfate		8-DEA tC DS (TT, D_2O)	
Absorbance (380 nm)	Integrated Emission	Absorbance (380 nm)	Integrated Emission
0.095	2.56E+08	0.065	9.65E+06
0.078	2.32E+08	0.052	7.33E+06
0.068	2.10E+08	0.046	6.20E+06
0.044	1.61E+08	0.041	4.73E+06
0.033	1.30E+08	0.035	3.74E+06
0.021	9.33E+07	0.024	2.12E+06

Figure S27. Quantum Yield determination plot and data table of 8-DEA tC DS (TT) in D_2O at 23°C.

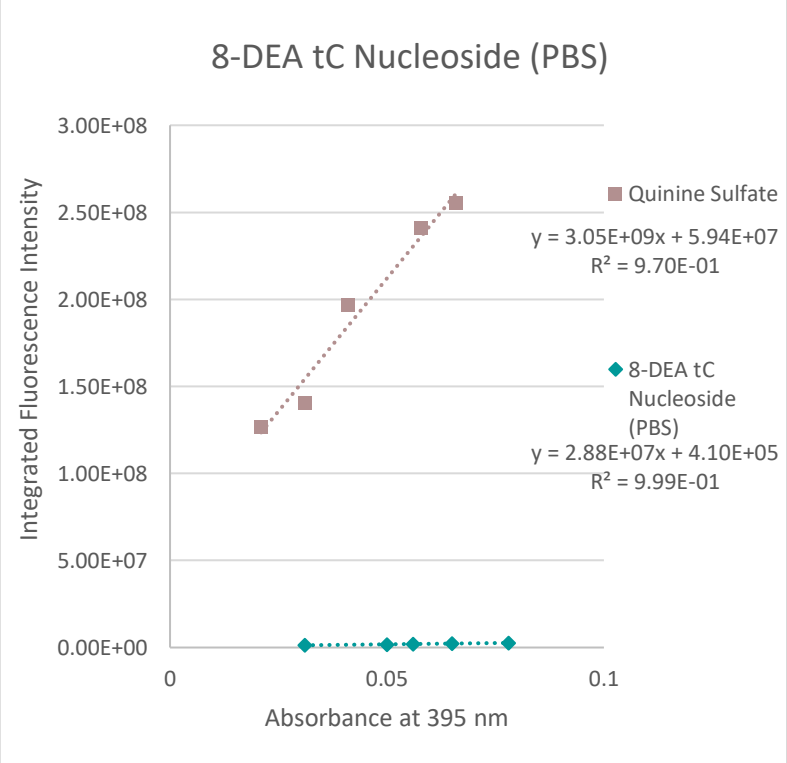

Quinine Sulfate		8-DEA tC Nucleoside (PBS)	
Absorbance (395 nm)	Integrated Emission	Absorbance (395 nm)	Integrated Emission
0.066	2.55E+08	0.078	2.66E+06
0.058	2.41E+08	0.065	2.27E+06
0.041	1.97E+08	0.056	2.04E+06
0.031	1.40E+08	0.050	1.84E+06
0.021	1.27E+08	0.031	1.30E+06

Figure S28. Quantum Yield determination plot and data table of 8-DEA tC (Nucleoside) in 1X PBS Buffer at 23°C.

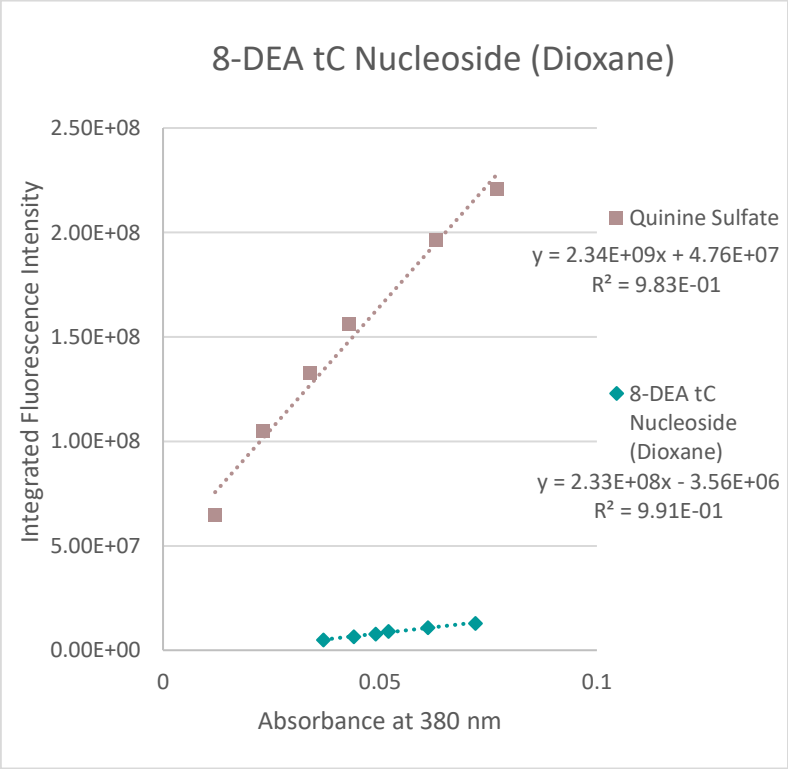

Quinine Sulfate		8-DEA tC Nucleoside (Dioxane)	
Absorbance (380 nm)	Integrated Emission	Absorbance (380 nm)	Integrated Emission
0.077	2.21E+08	0.072	1.30E+07
0.063	1.96E+08	0.061	1.09E+07
0.043	1.56E+08	0.052	9.00E+06
0.034	1.33E+08	0.049	7.80E+06
0.023	1.05E+08	0.044	6.53E+06
0.012	6.46E+07	0.037	4.96 E+06

Figure S29. Quantum Yield determination plot and data table of 8-DEA tC (Nucleoside) in Dioxane at 23°C.

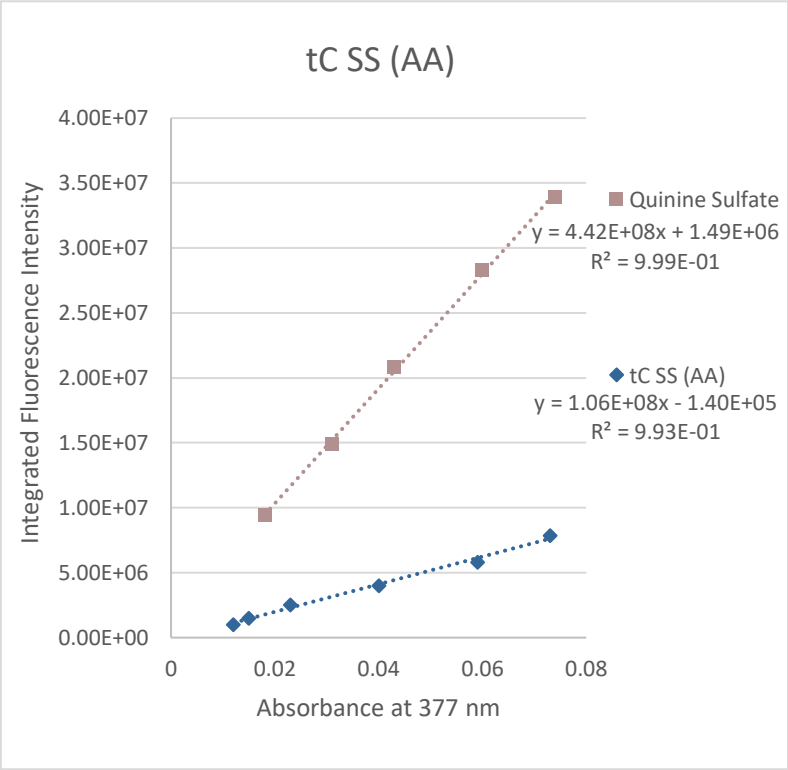

Quinine Sulfate		tC SS (AA)	
Absorbance (377 nm)	Integrated Emission	Absorbance (377 nm)	Integrated Emission
0.074	3.39E+07	0.073	7.87+06
0.060	2.83E+07	0.059	5.80E+06
0.043	2.08E+07	0.040	4.02E+06
0.031	1.49E+07	0.023	2.54E+06
0.018	9.43E+06	0.015	1.50E+06
		0.012	1.02E+06

Figure S30. Quantum Yield determination plot and data table of tC SS (AA) in 1X PBS Buffer at 23°C.

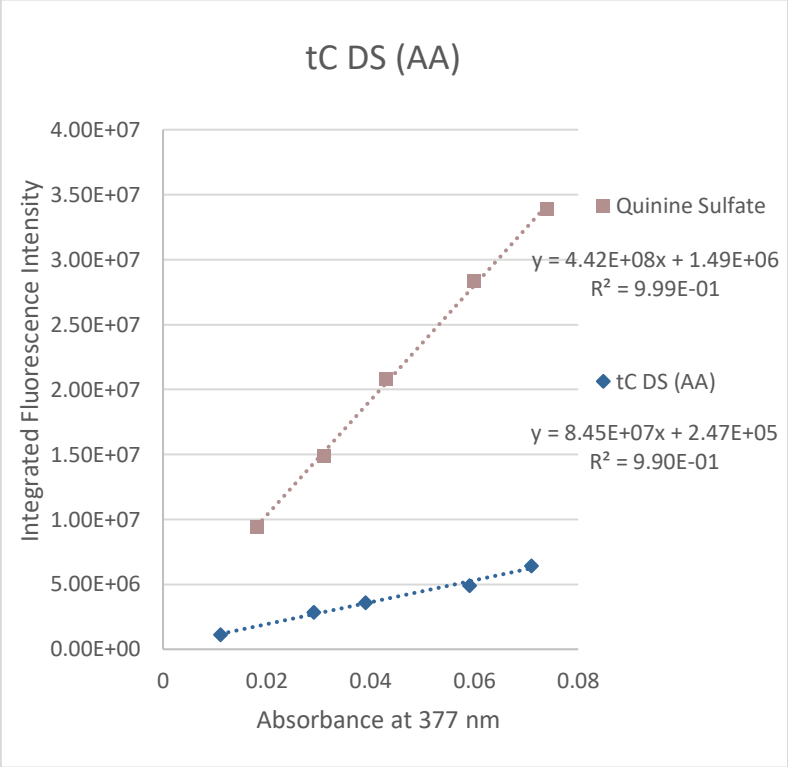

Quinine Sulfate		tC DS (AA)	
Absorbance (377 nm)	Integrated Emission	Absorbance (377 nm)	Integrated Emission
0.074	3.39E+07	0.071	6.43+06
0.060	2.83E+07	0.059	4.91E+06
0.043	2.08E+07	0.039	3.59E+06
0.031	1.49E+07	0.029	2.85+06
0.018	9.43E+06	0.011	1.11E+06

Figure S31. Quantum Yield determination plot and data table of tC DS (AA) in 1X PBS Buffer at 23°C.

Viscosity Sensitivity Measurements

The responsiveness of (8-DEA)tC, tC, and 9-(2,2-dicyanovinyl)julolidine (DCVJ) to viscosity changes using binary methanol-glycerol mixtures was determined.

Molecular rotors are known to have fluorescent properties that are dependent on the medium viscosity, the fluorescence spectra of parent **tC** and **(8-DEA)tC** were examined in methanol-glycerol mixtures ranging from 0 to 100% methanol in glycerol at 25 °C. These spectra were compared to a known molecular rotor **DCVJ** with well characterized properties.

Viscosity [cp] was calculated using equation

$\log \eta_{mix} = x_1 \log \eta_1 + x_2 \log \eta_2$

η: Solvent viscosity x_n: Volume fractions of each solvent

The preparation of ten separate samples of the same concentrations with varying binary viscosity mixtures of MeOH:Glycerol were prepared. Special care had to be taken in the preparation of the mixtures that contained 50% Glycerol and above. Due to its very viscous nature heat was applied (~45°C) for about 1 hr to aid in the thorough mixing of the solution being studied. In general a stock solution of the compound was prepared in DMSO and a known volume was added to each of the binary mixtures. In all cases background spectra were recorded and subtracted from the resulting spectra.

All experiments are ran in duplicate and an average slopes is reported herein

The solvent mixtures span a viscosity range from 0.538 cP to 1317 cP.

A calibration plot of fluorescence intensity (I) versus viscosity (η) were constructed using the Foster-Hoffman equation $\Phi_F = z\eta^{\alpha}$, relating the fluorescence quantum yield (Φ_F) as a function of viscosity (η) and fluorophore and solvent-specific constants (z, α).

The simplified relationship:

$\log(I) = C + x\log(\eta)$

I: fluorescence emission intensity η: solvent viscosity

X: dye-dependent constant C: temperature-dependent constant

Derived from the Foster-Hoffman relation, a clear correlation between fluorescence intensity and viscosity of the solvent mixture was established. The viscosity of the sample seemed to have a minimal impact on the compounds absorbance spectra with greater implications in the fluorescence spectra.

Viscosity of binary methanol-glycerol mixtures

Volume Ratio Methanol: Glycerol	Viscosity [cp]
1:0	0.583
0.9:0.1	1.84

0.8:0.2	5.14
0.7:0.3	13.03
0.6:0.4	30.27
0.5:0.5	65.27
0.4:0.6	131.85
0.3:0.7	251.50
0.2:0.8	456.01
0.1:0.9	790.60
0:1	1317.00

Parent tC

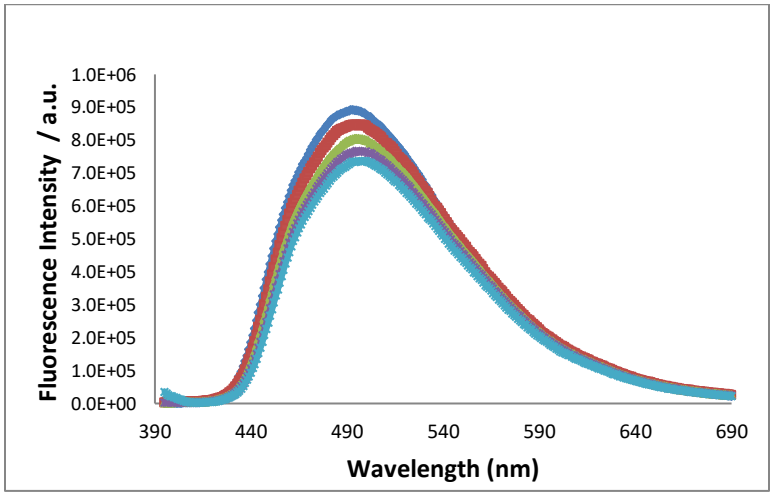

Figure S32. Emission of **parent tC** as a function of viscosity. Parent tC is effectively insensitive to solvent viscosity. Excitation at 377nm, 5nm excitation slit widths, 0.5nm emission slit widths.

(8-DEA)tC compound (1)

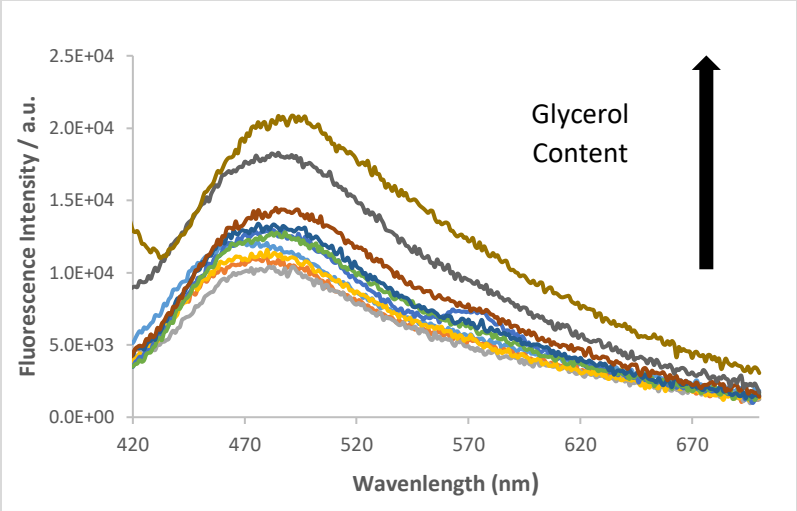

Figure S33. A) Emission of **8-DEA-tC** as a function of viscosity. Different samples of the same concentration of 8-DEA-tC were prepared for each binary mixture of glycerol and methanol. Excitation at 380nm, 10nm excitation slit widths, 0.5nm emission slit widths. Glycerol content (and therefore viscosity) correlates with an increase in fluorescence.

DCVJ

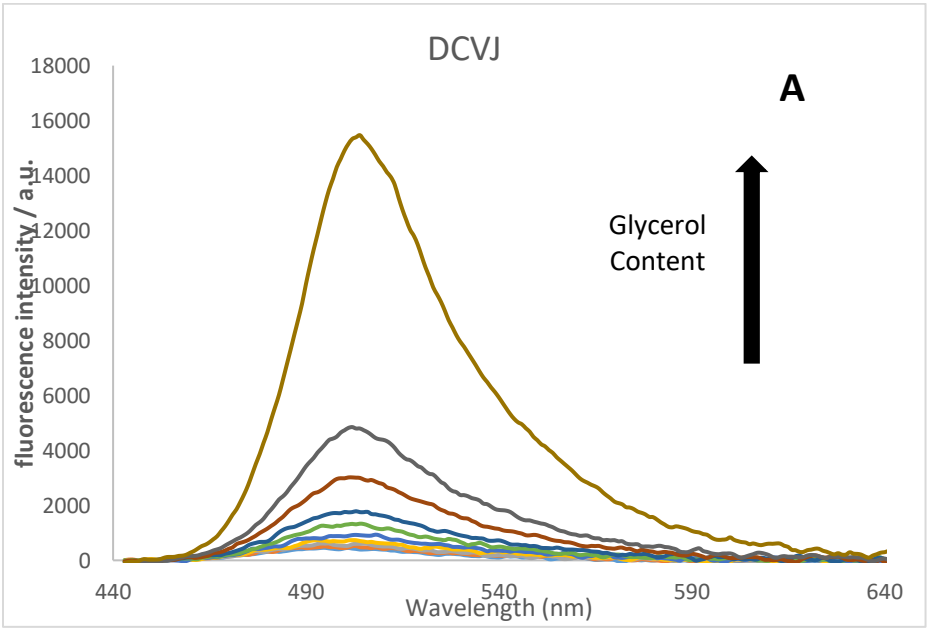

Figure S34. A) Emission of **DCVJ** as a function of viscosity. An increase in glycerol content resulted in a large increase in fluorescence emission. Differnet samples of the same concentration were prepared for each mixture of glycerol and methanol. DCVJ is an established molecular rotor and viscosity probe. Excitation at 433nm, emission and excitation slit widths 0.65nm

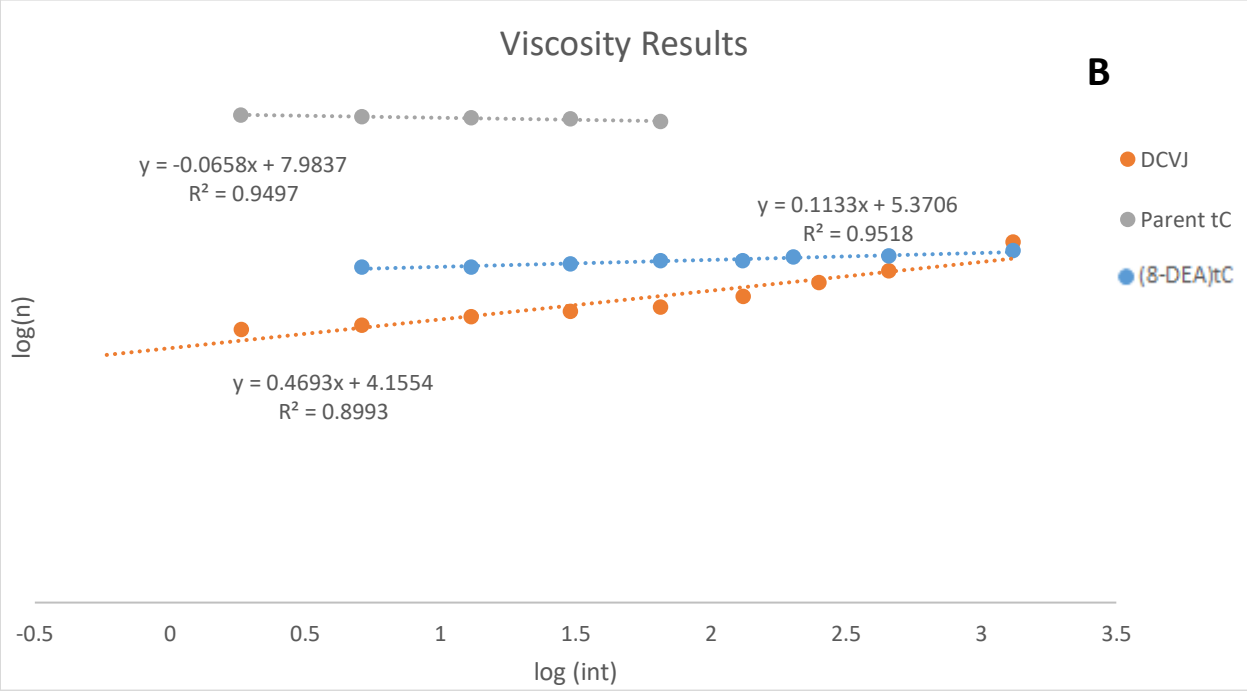

Figure S35. B) The integrated fluorescence intensity of **(8-DEA)tC, parent tC, and DCVJ** were plotted against log(η) and according to the Foster-Hoffman relation. The slope could be extracted which represents the viscosity sensitivity of the probes. Example data is plot above but all experiments were run at least in duplicate and averaged results are reported below.

Compound	Slope representing viscosity sensitivity x
DCVJ	0.45 ± 0.04
tC	−0.01 ± 0.04
8-DEA-tC	0.13 ± 0.04

6. Stern-Volmer Analysis

In order to assess the magnitude that chloride, present in our buffers, would quench the fluorescent cytidine analogues, a Stern-Volmer analysis was performed spanning from 0 mM NaCl to 180 mM NaCl to mimic the environment of the 1XPBS buffer used in the fluorescence measurements of the oligomers.

A solution of fluorophore was prepared and known volumes of 0.5 M NaCl solution were titrated in and the resulting fluorescence change was measured. The dilution factor was taken into account when calculating integrated fluorescence intensity.

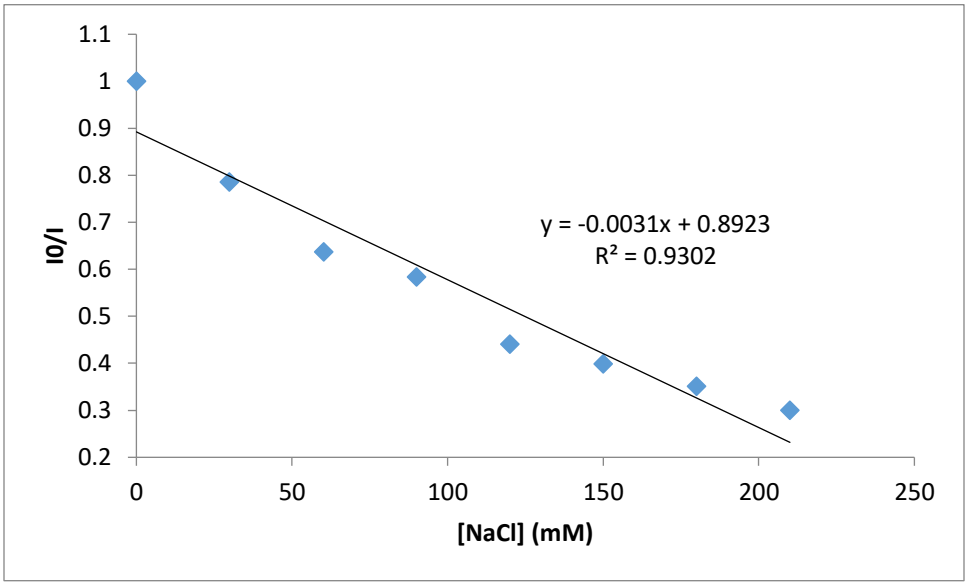

Figure S36. Example plot of (8-DEA)tC nucleoside I_o/I plotted against [NaCl], fluorescence intensity increased as a function of [NaCl] in mM. Excitation at 380nm, 10nm excitation slit widths, 0.5nm emission slit widths. Experiments were run in duplicate and an average value of the Stern-Volmer constant $K_{SV} = -3.1 \pm 0.4\ M^{-1}$ was obtained.

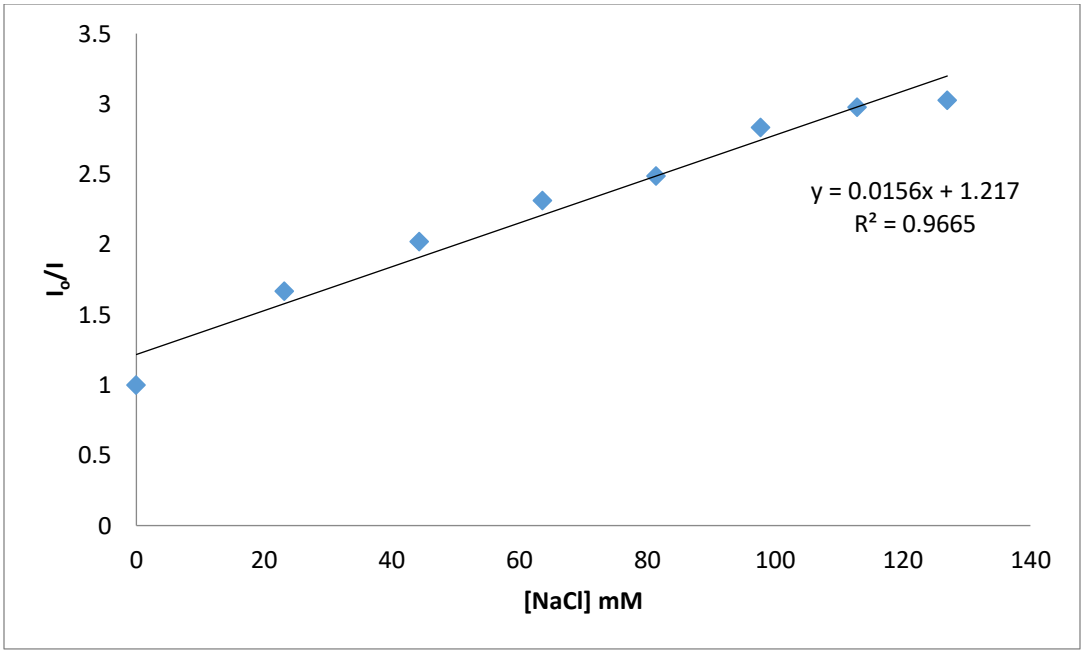

Figure S37. Example plot of (8-DEA)tC duplex oligonucleotide **TT**; I_o/I plotted against [NaCl] in mM; fluorescence intensity decreased as a function of [NaCl]. Excitation at 380nm, 10nm excitation slit widths, 0.5nm emission slit widths. Experiments were run in duplicate and an average value of the Stern-Volmer constant K_{SV} = 12.7 ± 2 M^{-1} was obtained.

7. Circular dichroism and melting temperature measurements

UV CD spectra of oligonucleotide duplexes at a concentration of 5 µM in phosphate buffered saline (10 mM sodium phosphate, pH 7.4, 27 mM potassium chloride, 137 mM sodium chloride) were collected at 25°C in a 1 cm path length cell on an Aviv model 420 spectrophotometer equipped with a Peltier temperature controller. Background-subtracted spectra were smoothed and normalized to concentration using A_{260nm} as calculated from detector voltage using the following equation and converted to standard units.

$$\text{Abs} = \log\left(\frac{\text{Voltage}_{\text{sample}}}{\text{Voltage}_{\text{solvent}}}\right) * 7.4$$

Elipticity at 255 nm was monitored from 15ºC to 75ºC at 1ºC increments. The T_M of each duplex was calculated by fitting the raw data to a two-state model in Igor Pro. Melting curves are reported as fraction unfolded.

$$\alpha_U = \frac{\theta_i - \theta_F}{\theta_U - \theta_F}$$

Where θ is ellipticity in mdeg and subscripts U and F indicate signals of strand-separated and duplex DNA, respectively.

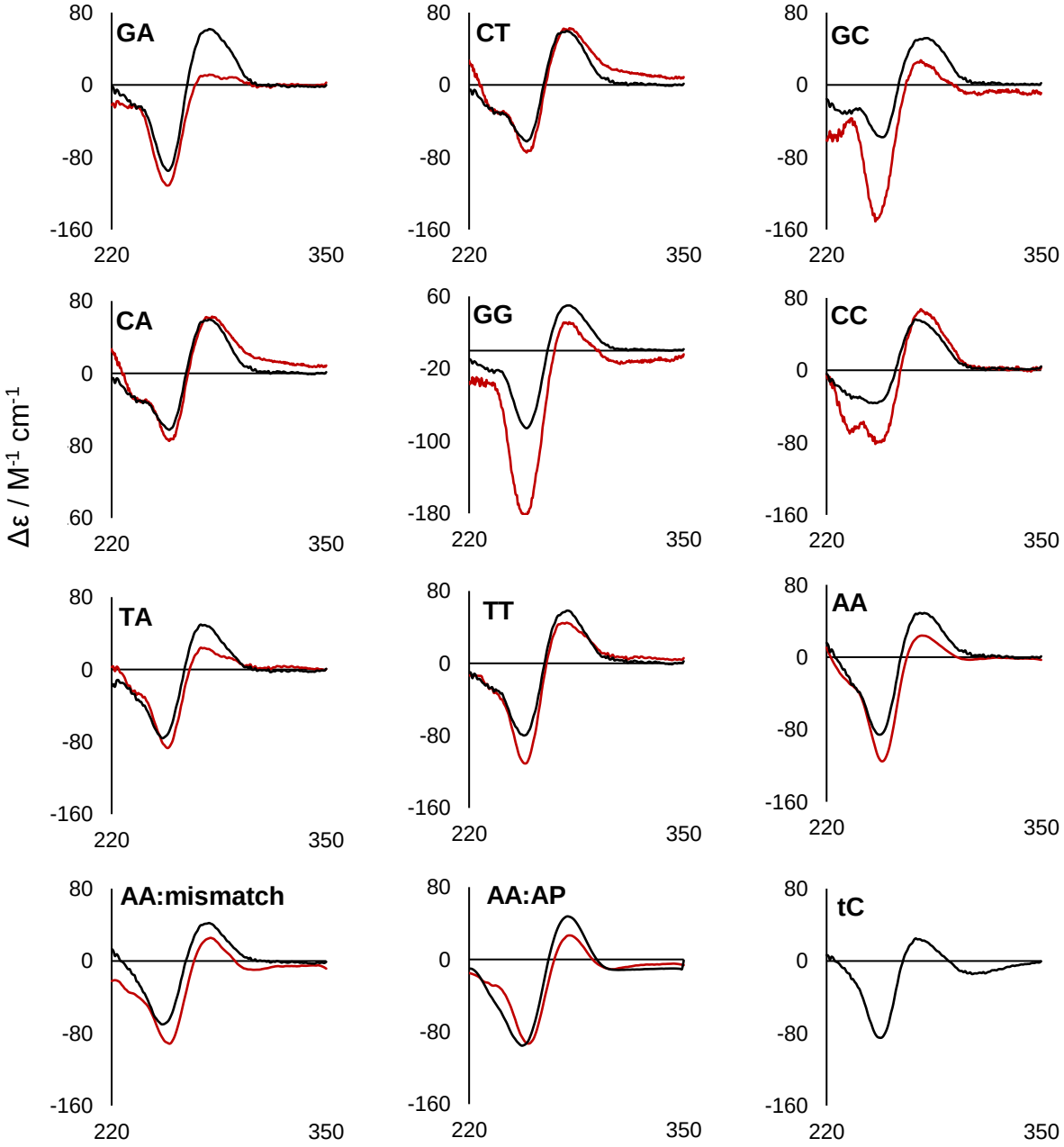

Figure S38. CD Spectra of duplex oligonucleotides at 5 µM in 1X PBS from 350 to 220 nm. Oligonucleotide duplexes incorporating 8-DEA-tC (red) or cytosine (black) and neighboring 5′ and 3′ bases as named in the main text. The bottom right panel is of the duplex containing tC and neighboring bases AA.

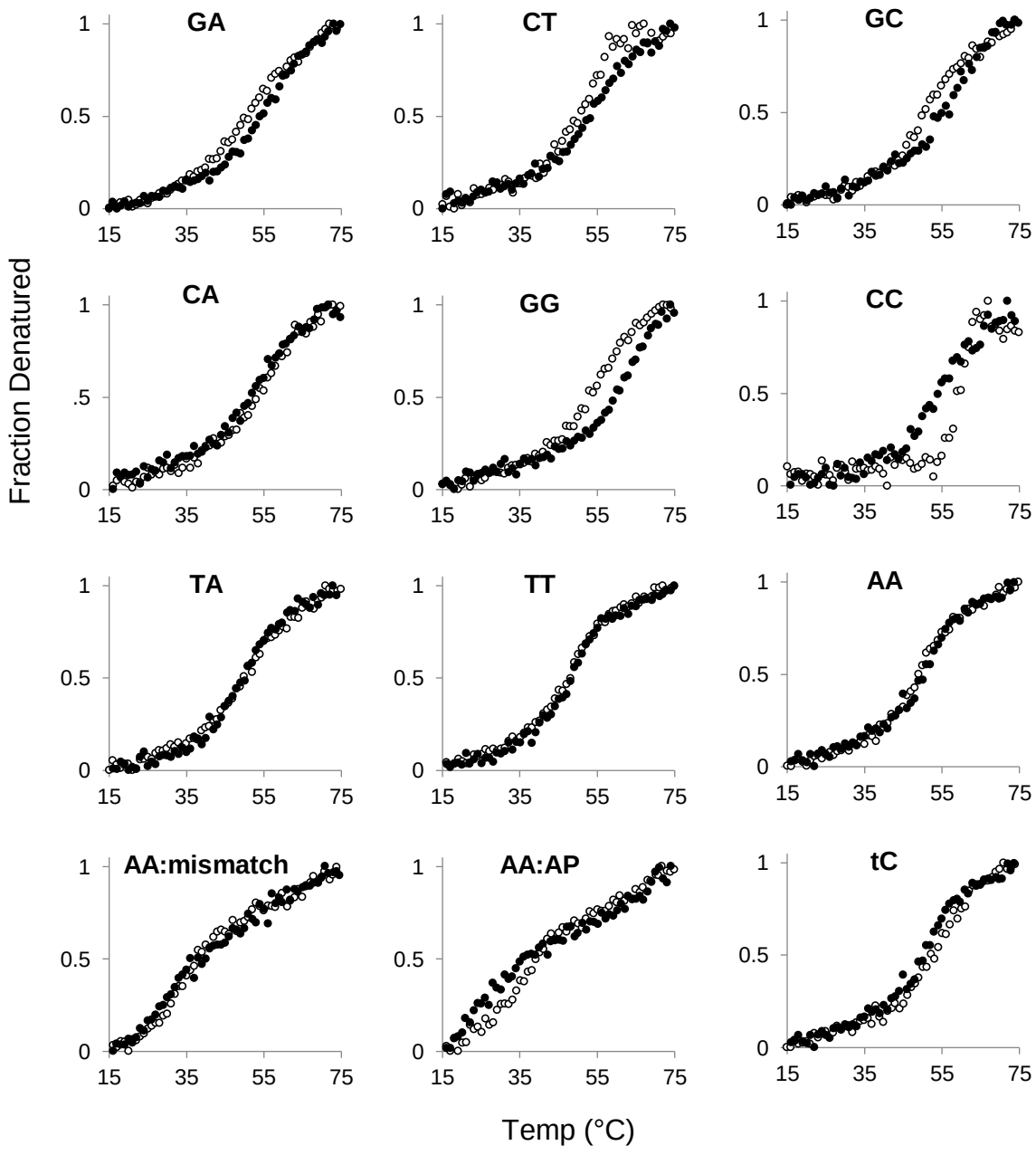

Figure S39. CD melting curves at 255 nm for 8-DEA-tC oligonucleotides (open circles) and native DNA duplexes (closed circles). tC is plotted next to native AA.

8. NMR Spectra

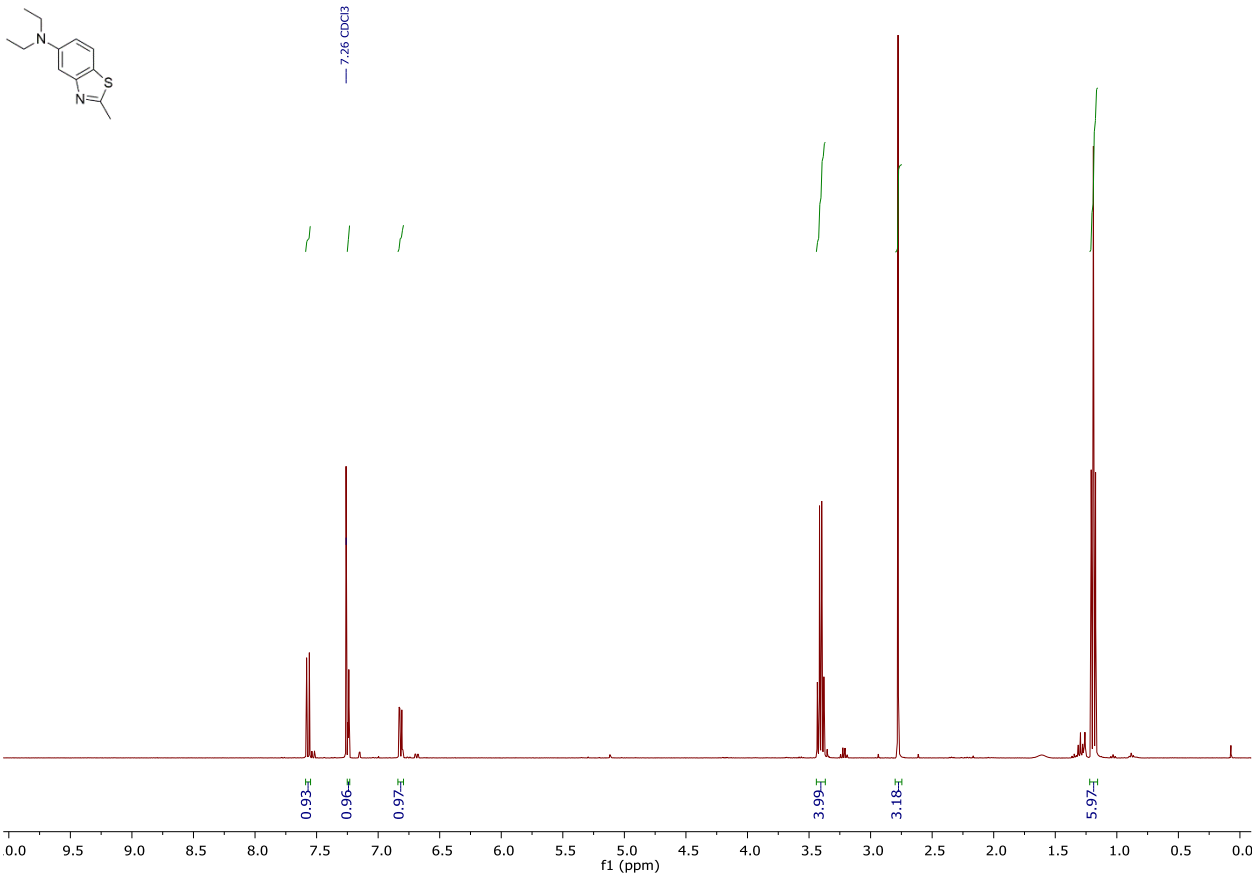

Figure S40: ^{1}H NMR spectra of 5-diethylamino-2-methylbenzothiazole **7.** Spectrum acquired at 298K, $CDCl_3$, 400 MHz

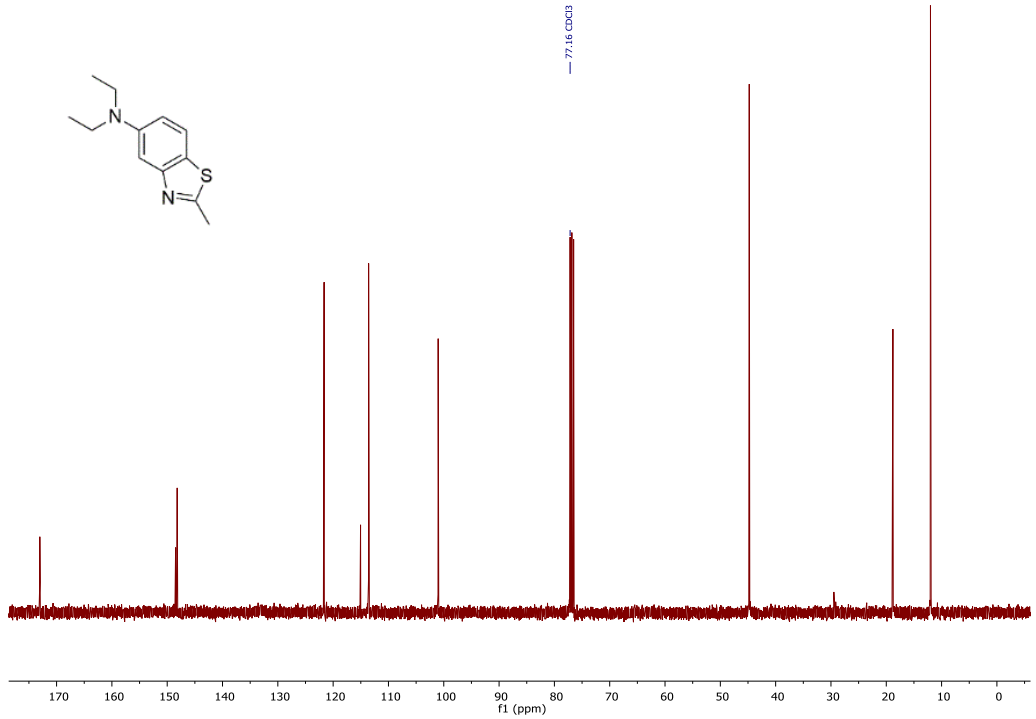

Figure S41: ^{13}C NMR of 5-Diethylamino-2-methylbenzothiazole **7.** Spectrum acquired at 298K, $CDCl_3$, 100 MHz

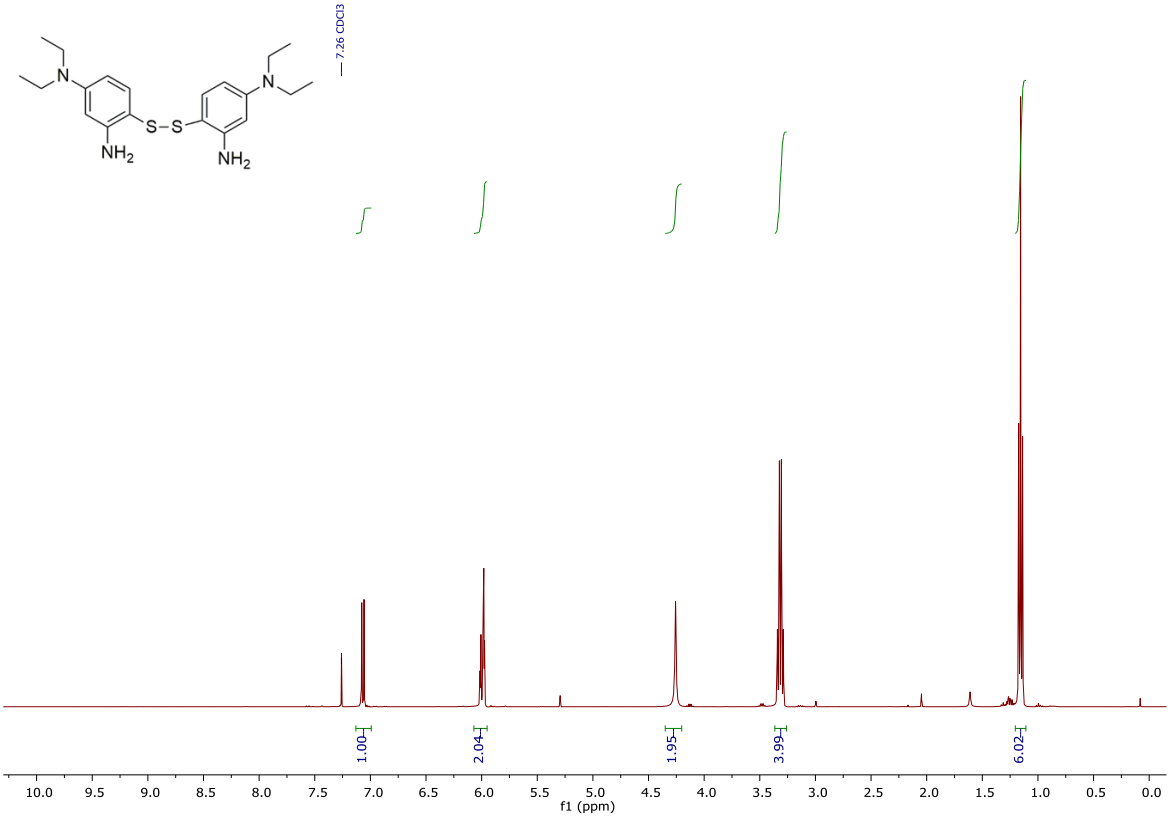

Figure S42: ^{1}H NMR of 2-[(2-Amino-4-diethylaminophenyl)disulfanyl]-5-diethylaminoaniline **3.** Spectrum acquired at 298K, $CDCl_3$, 400 MHz

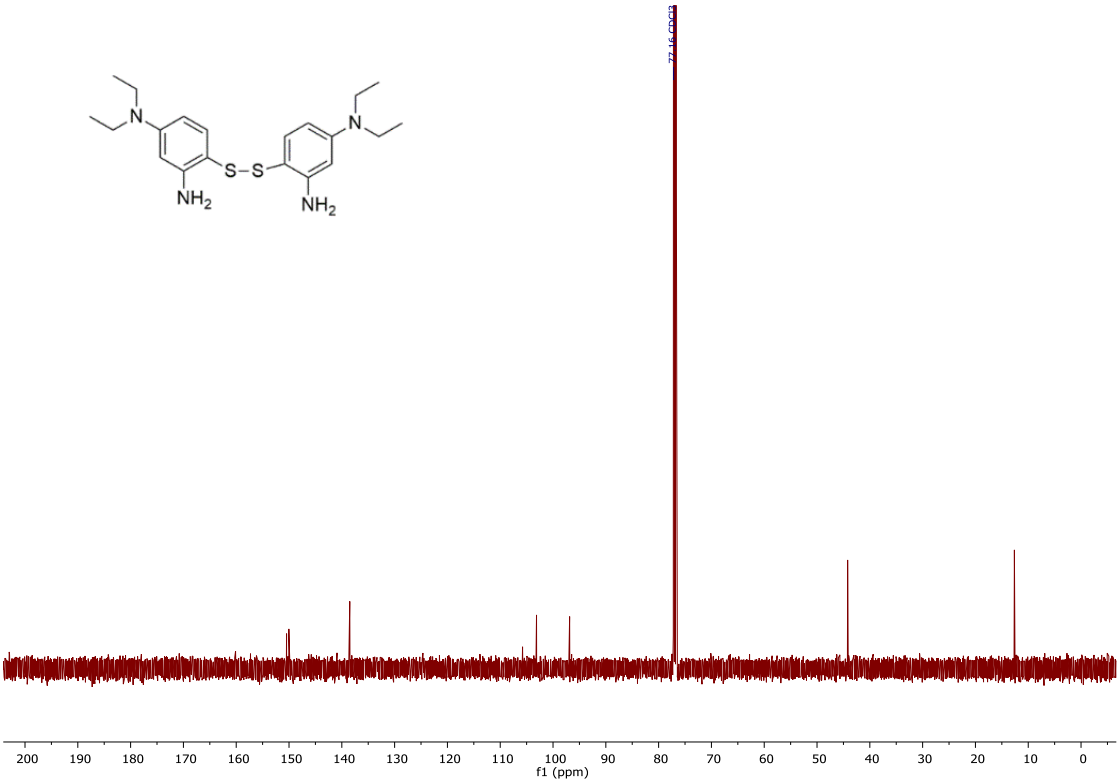

Figure S43: ^{13}C NMR of 2-[(2-Amino-4-diethylaminophenyl)disulfanyl]-5-diethylaminoaniline **3.** Spectrum acquired at 298K, $CDCl_3$, 100 MHz

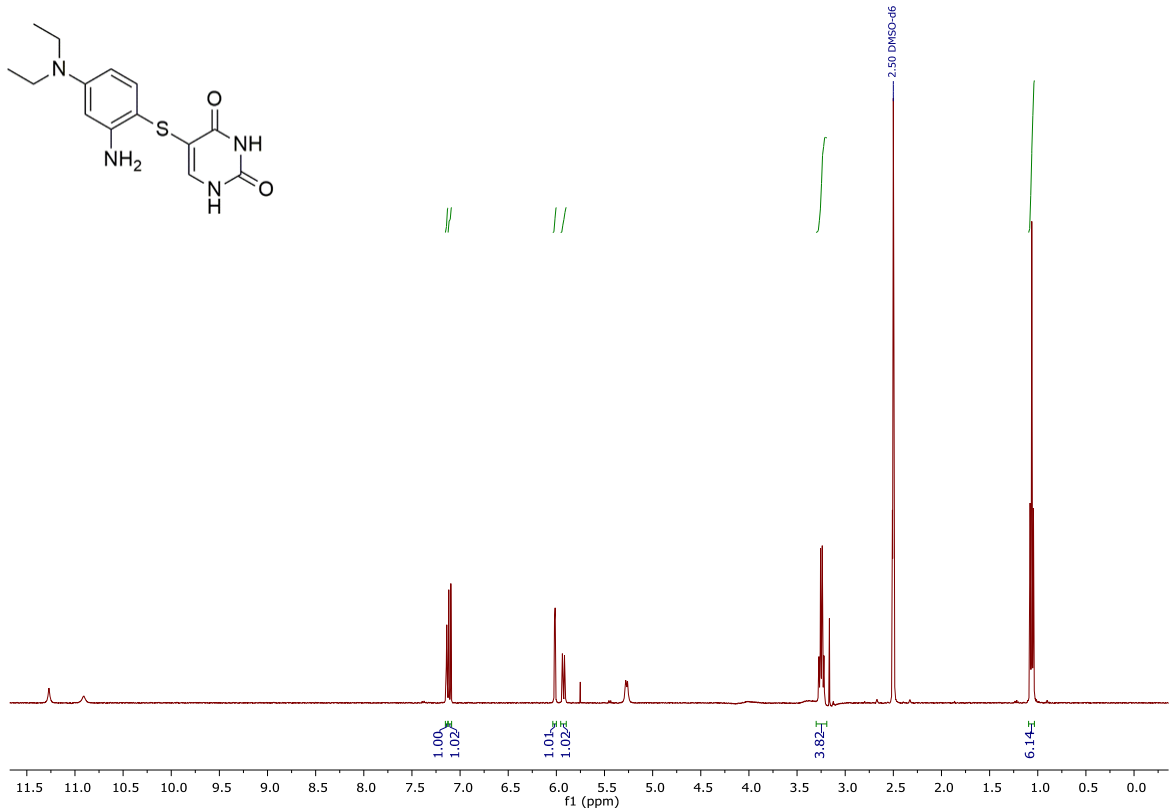

Figure S44: ^{1}H NMR 5-[(2-Amino-4-diethylaminophenyl)sulfanyl]pyrimidine-2,4(1*H*,3*H*)-dione **4.** Spectrum acquired at 298K, d-DMSO, 400 MHz

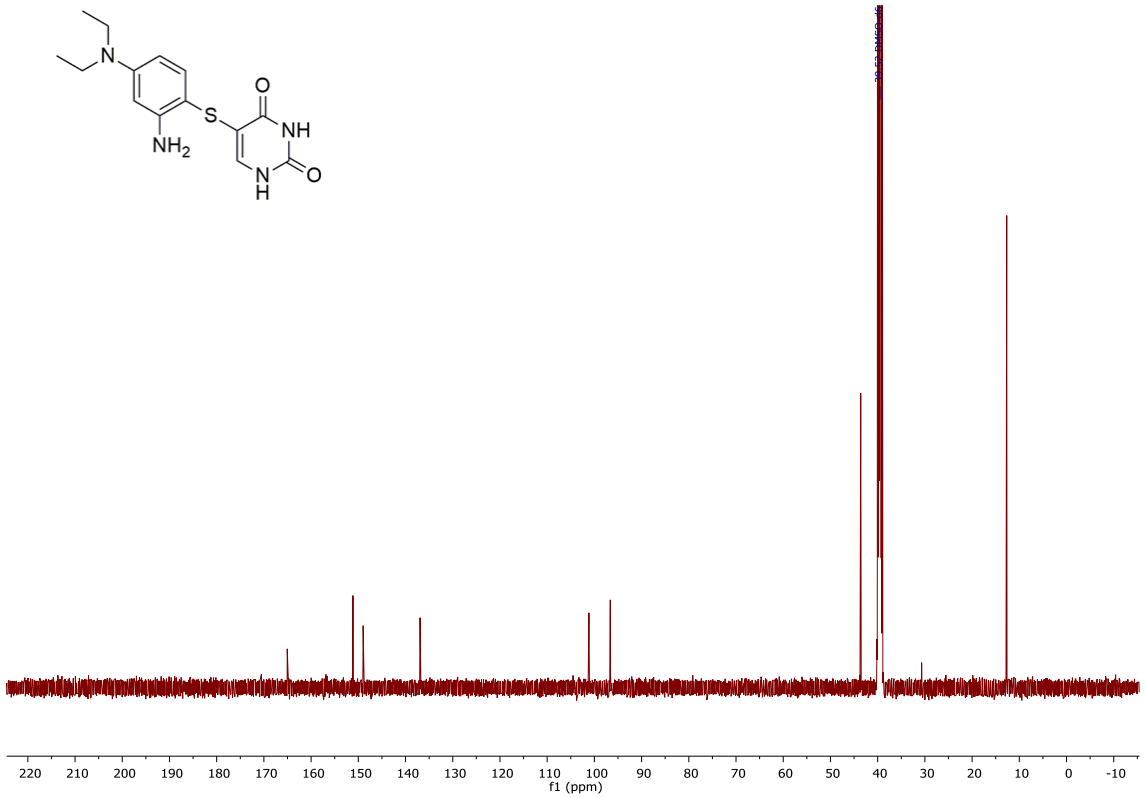

Figure S45: ^{13}C NMR of 5-[(2-Amino-4-diethylaminophenyl)sulfanyl]pyrimidine-2,4(1*H*,3*H*)-dione **4.** Spectrum acquired at 298K, d-DMSO, 100 MHz

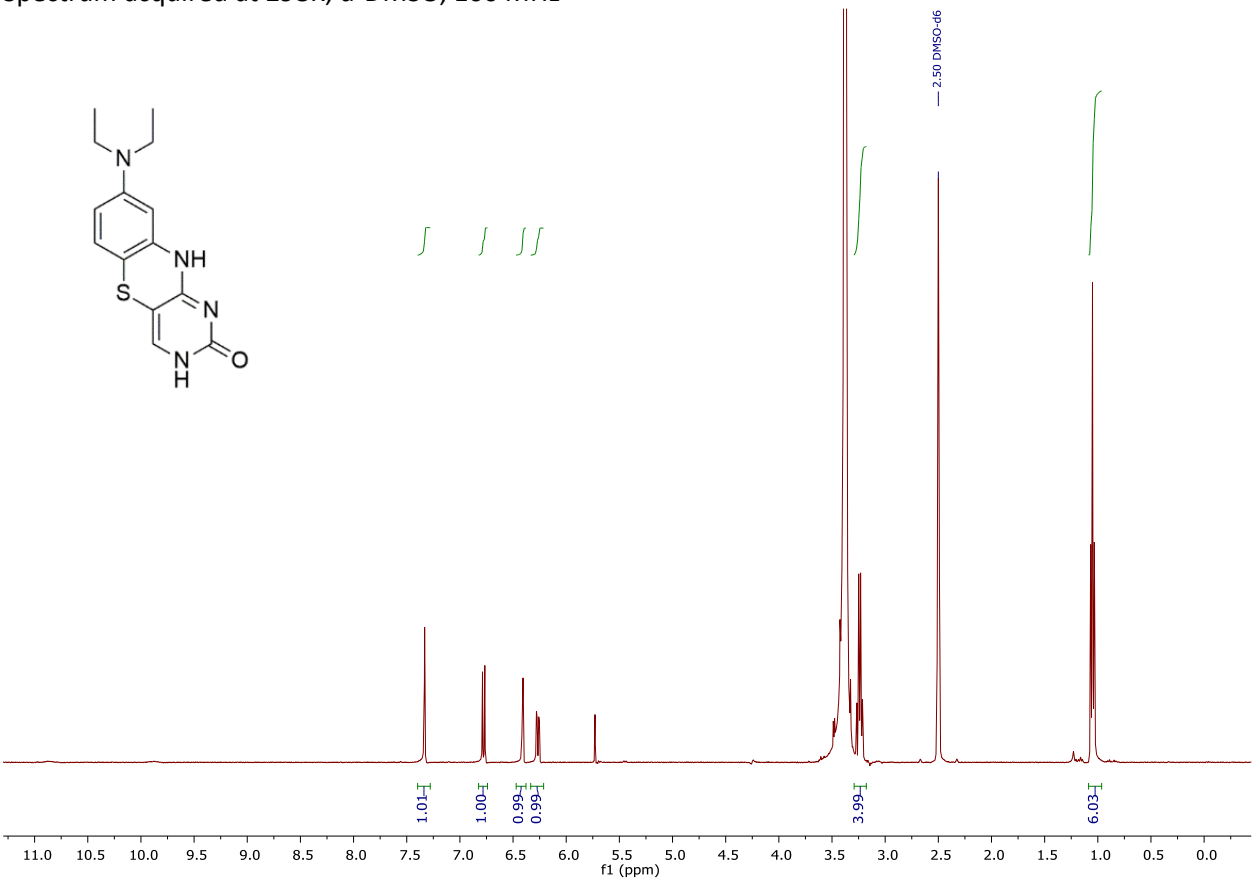

Figure S46: ^{1}H NMR of 8-Diethylamino-3*H*-pyrimido[5,4-*b*][1,4]benzothiazin-2(10*H*)-one **5.** Spectrum acquired at 298K, d-DMSO, 400 MHz

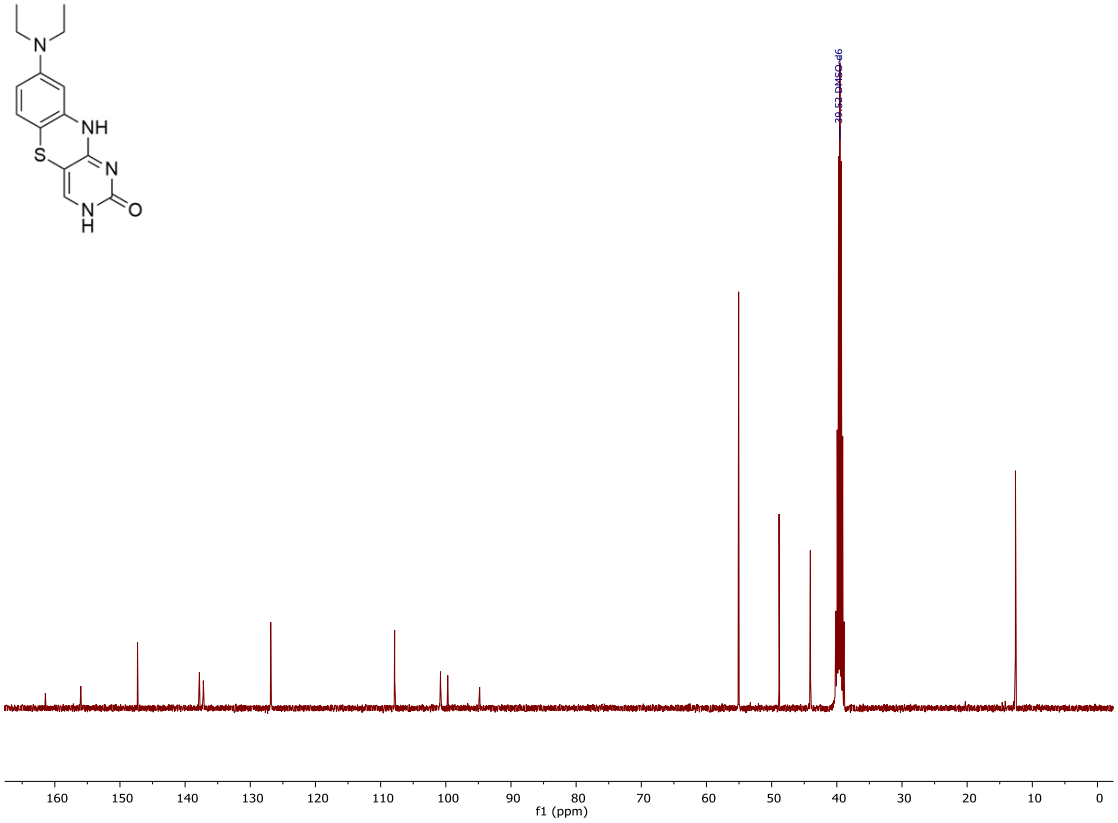

Figure S47: ^{13}C NMR of 8-Diethylamino-3*H*-pyrimido[5,4-*b*][1,4]benzothiazin-2(10*H*)-one **5.** Spectrum acquired at 298K, d-DMSO, 100 MHz

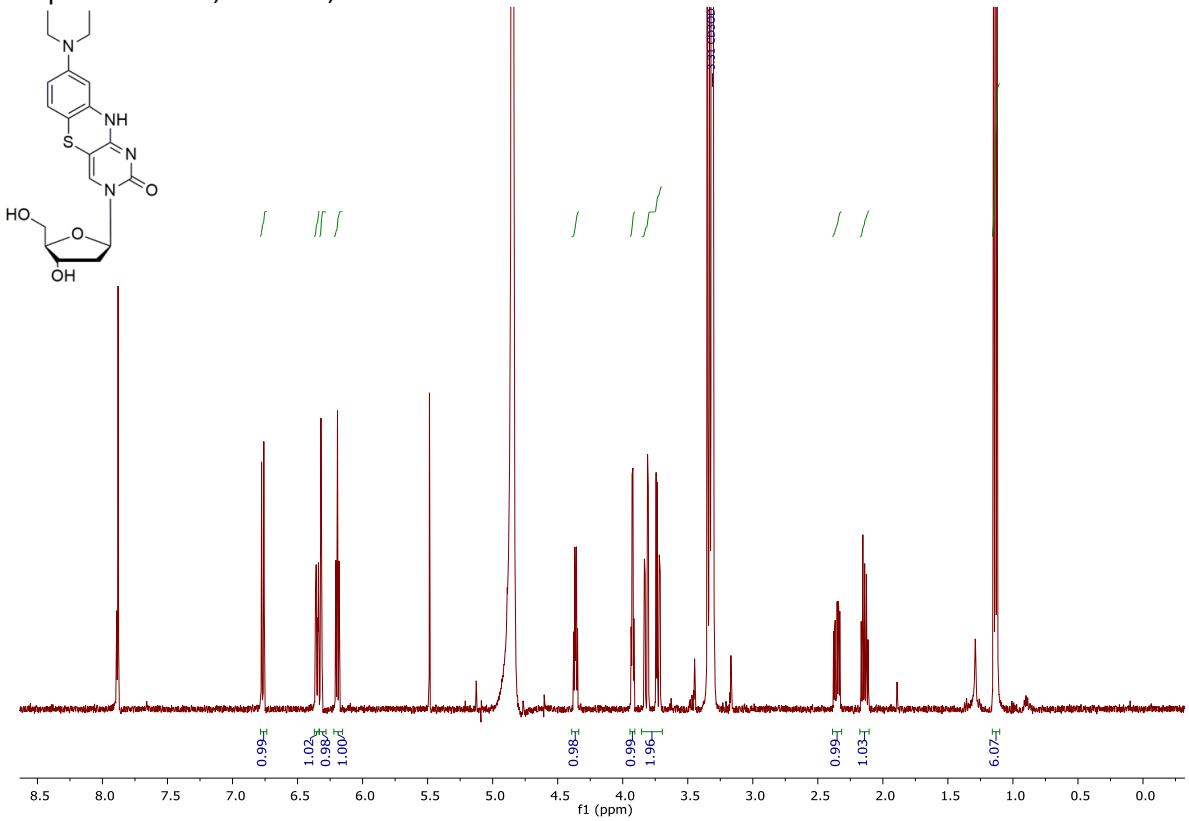

Figure S48: ^{1}H NMR of 8-Diethylamino-tricyclic-2'-deoxy-*β*-D-ribonucleoside **1.** Spectrum acquired at 298K, MeOD, 400 MHz

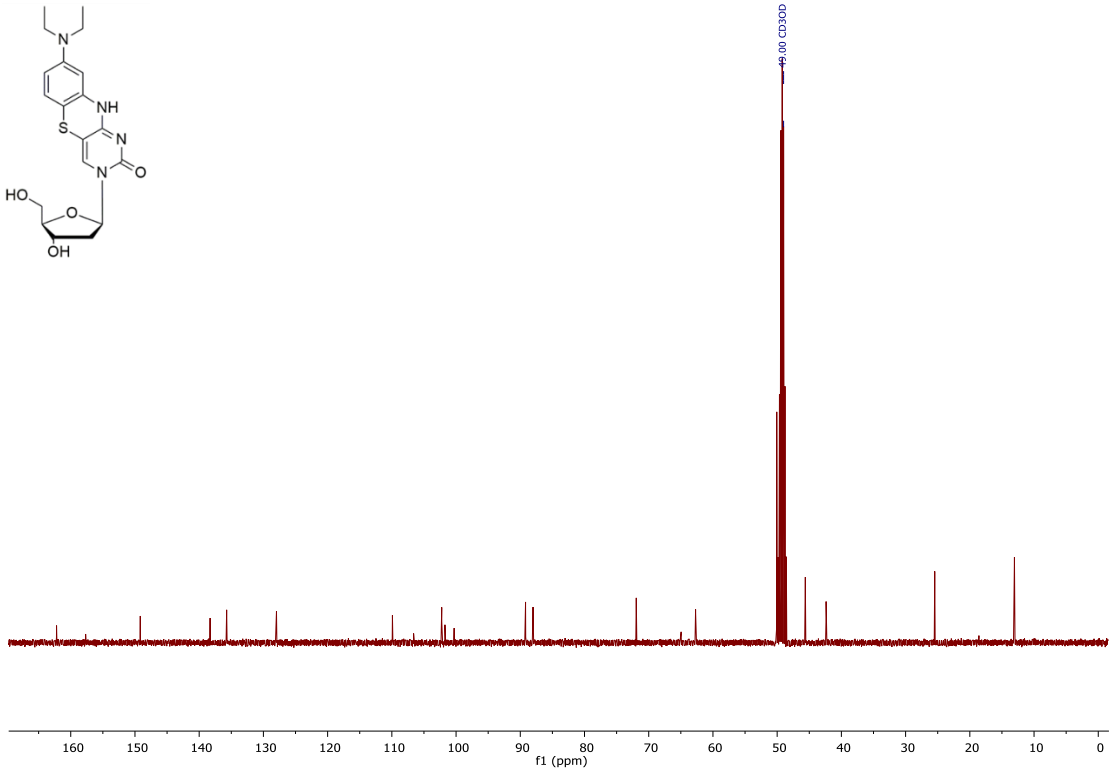

Figure S49: ^{13}C NMR of 8-Diethylamino-tricyclic-2'-deoxy-*β*-D-ribonucleoside **1.** Spectrum acquired at 298K, MeOD, 100 MHz

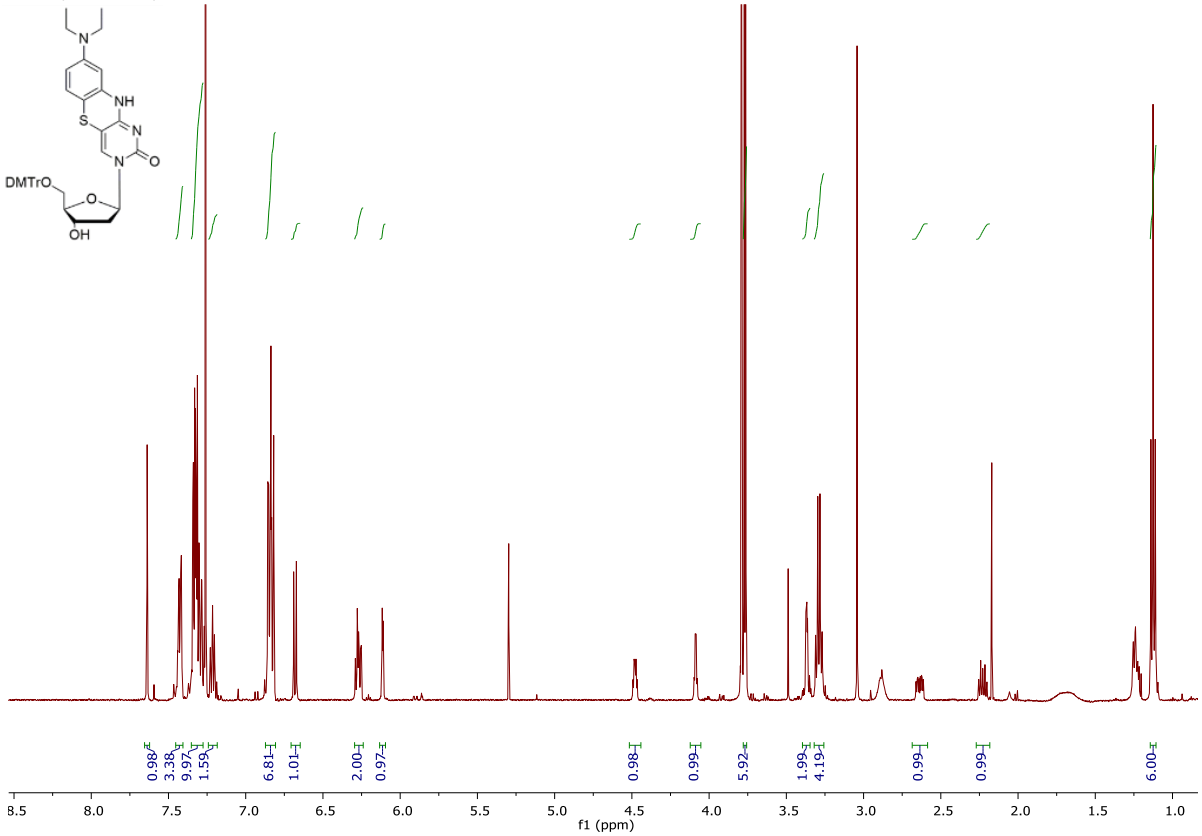

Figure S50: ^{1}H NMR of 8-Diethylamino-tC 2'-deoxy-5'-dimethoxytrityl-*β*-D-ribonucleoside **9.** Spectrum acquired at 298K, $CDCl_3$, 400 MHz

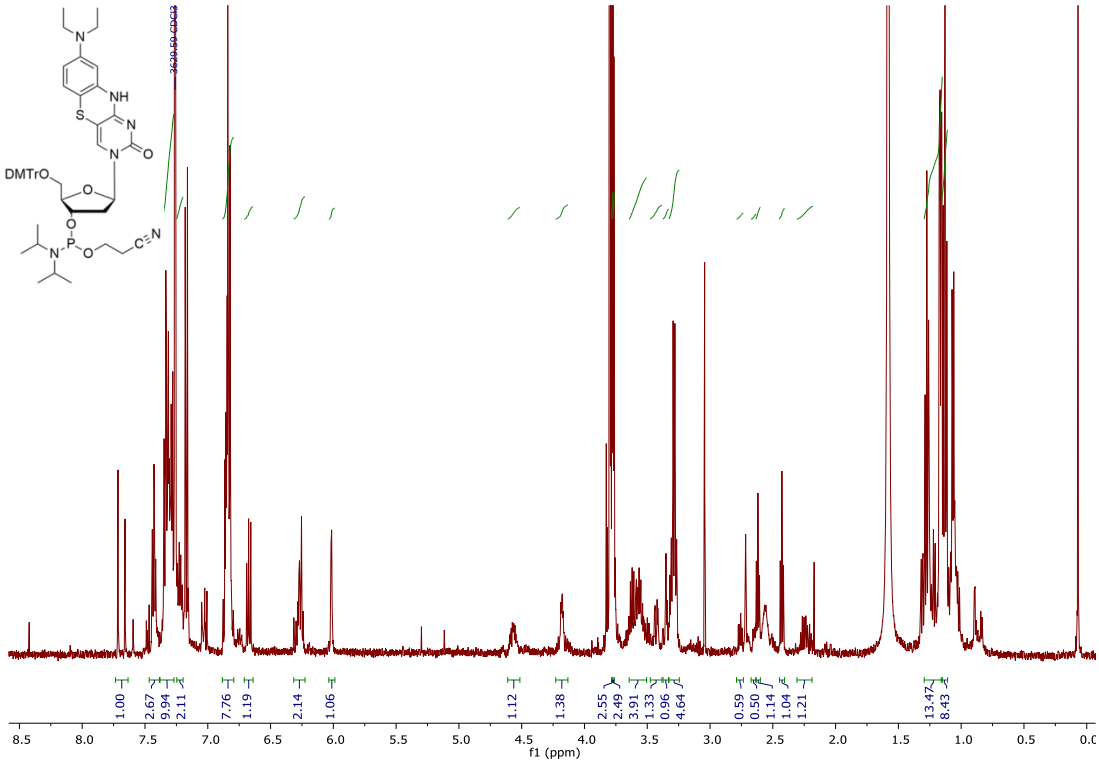

Figure S51: ^{1}H NMR of 8-Diethylamino-tC 2'-deoxy-5'-dimethoxytrityl-3'-cyanoethyldiisopropylphosphoramidite-*β*-D-ribonucleoside **10.** Spectrum acquired at 298K, $CDCl_3$, 400 MHz

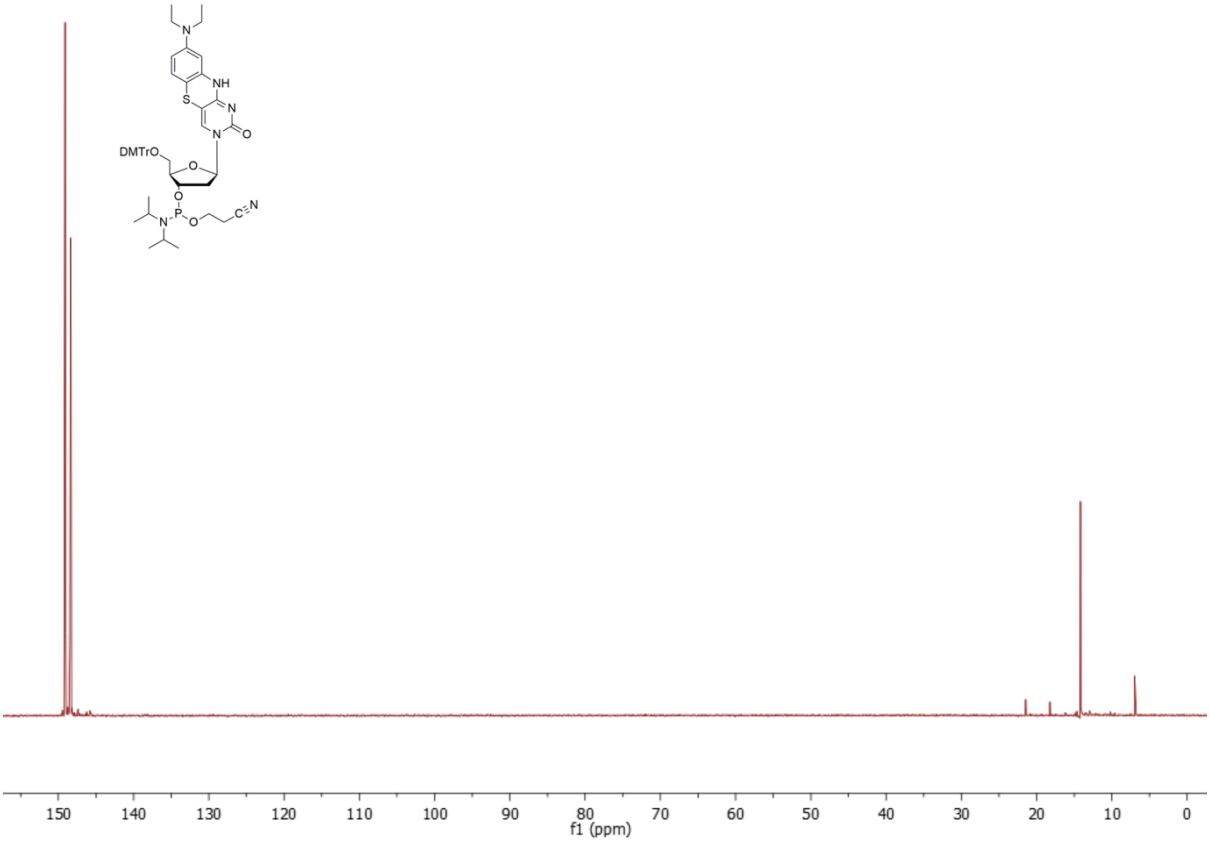

Figure S52: ^{31}P NMR of 8-Diethylamino-tC 2'-deoxy-5'-dimethoxytrityl-3'-cyanoethyldiisopropylphosphoramidite-*β*-D-ribonucleoside **10** Spectrum acquired at 298K, $CDCl_3$, 162 MHz.

9. References

[1] GAUSSIAN 09, Revision D.01, Frisch, M. J.; Trucks, G. W.; Schlegel, H. B.; Scuseria, G. E.; Robb, M. A.; Cheeseman, J. R.; Scalmani, G.; Barone, V.; Mennucci, B.; Petersson, G. A.; Nakatsuji, H.; Caricato, M.; Li, X.; Hratchian, H. P.; Izmaylov, A. F.; Bloino, J.; Zheng, G.; Sonnenberg, J. L.; Hada, M.; Ehara, M.; Toyota, K.; Fukuda, R.; Hasegawa, J.; Ishida, M.; Nakajima, T.; Honda, Y.; Kitao, O.; Nakai, H.; Vreven, T.; Montgomery, J. A., Jr.; Peralta, J. E.; Ogliaro, F.; Bearpark, M.; Heyd, J. J.; Brothers, E.; Kudin, K. N.; Staroverov, V. N.; Kobayashi, R.; Normand, J.; Raghavachari, K.; Rendell, A.; Burant, J. C.; Iyengar, S. S.; Tomasi, J.; Cossi, M.; Rega, N.; Millam, J. M.; Klene, M.; Knox, J. E.; Cross, J. B.; Bakken, V.; Adamo, C.; Jaramillo, J.; Gomperts, R.; Stratmann, R. E.; Yazyev, O.; Austin, A. J.; Cammi, R.; Pomelli, C.; Ochterski, J. W.; Martin, R. L.; Morokuma, K.; Zakrzewski, V. G.; Voth, G. A.; Salvador, P.; Dannenberg, J. J.; Dapprich, S.; Daniels, A. D.; Farkas, Ö.; Foresman, J. B.; Ortiz, J. V.; Cioslowski, J.; Fox, D. J. Gaussian, Inc., Wallingford CT, 2009.

[2] Becke, A. D. *J. Chem. Phys.*, **98** (1993) 5648-5652.

[3] Lee, C.; Yang, W.; Parr, R. G. *Phys. Rev. B*, **37** (1988) 785-789.

[4] Dunning Jr., T. H. *J. Chem. Phys.*, **90** (1989) 1007-23.

[5] Foster, J. P.; Weinhold, F. *J. Am. Chem. Soc.*, **102** (1980) 7211-18.

[6] GAUSSVIEW, Version 5, Dennington, Roy; Keith, Todd; Millam, John. *Semichem Inc.*, Shawnee Mission, KS, 2009.

[7] Williams, A. T. R.; Winfield, S. A.; Miller, J. N. *Analyst* **108** (1983) 1067–1071.

[8] Noé, M. S.; Ríos, A. C.; Tor, Y. *Org. Lett.* **14** (2012) 3150–3153.